How do Laser Pointers Damage your Retina?

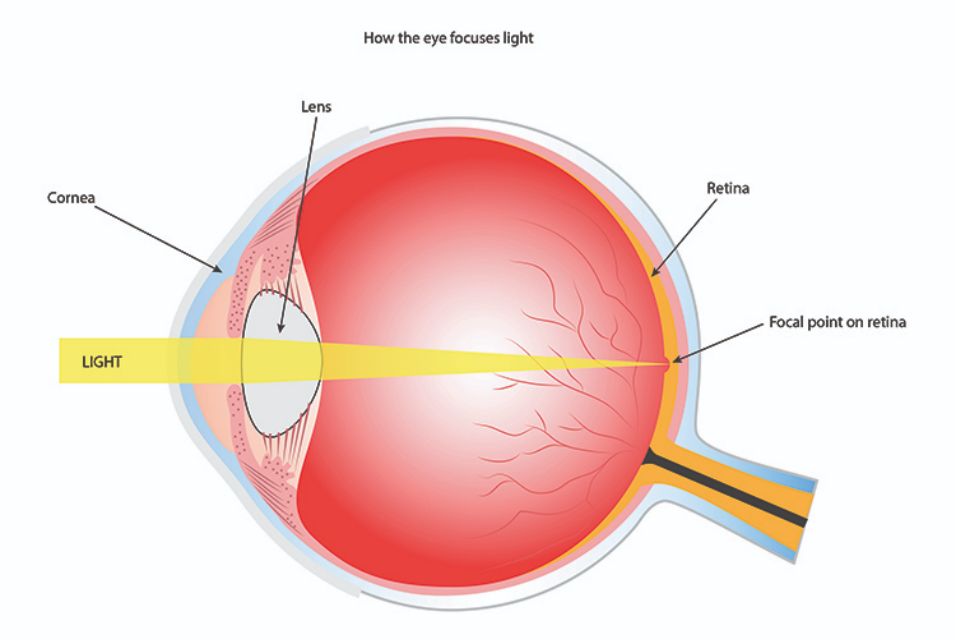

Keywords: Laser, Retina, Thermocoagulation, Human Eyeball, COMSOL

BEE 4530/MAE 5530: Computer Aided Engineering: Application to Biological Processes

1 Executive Summary

Lasers are devices used for many applications, for instance, in CD burning and reading, to baffle an audience in a light show or to point out details on a projector. The handheld laser or laser pointer is not given much thought, never mind that it could be seen as a dangerous object. And although the vast majority of market-available laser pointers are completely safe and even carry a warning, incidents occur. Goofing children or adults are seriously hurt due to over exposure to a laser device into their eyes, causing vision impairment that can last for life.

Although your eyes provide some natural protection against intense flashes of light, such as the blinking reflex, damage can occur before this sets in. Additionally, a person can be unaware that damage is being inflicted onto the retinal region of their eyes and therefore continue looking into the laser. In some scenarios, the label on the laser does not correspond to the actual power of a laser and therefore it can be hard to know what lasers are safe and for which laser you need protective gear.

In this project, we will be exploring damage caused by a visible spectrum laser to the retina of a human eye. We will investigate the thresholds of time and laser power before thermal damage to the retina is caused. To this end, we will be using a 2D axisymmetric model of the retina undergoing heating through a laser at a fixed point. We will be analyzing several factors that can determine the extent of thermal damage to the retina and will analyze different wavelengths or colors of visible spectrum laser light.

Through changing parameters, we have found that wider beams are safer compared to more narrow beams as the power output of these lasers is less condensed. Furthermore, it is shown that power is linearly proportional to the heating of the retinal region. Additionally it is shown that cornea thickness, which is related to age, as elderly people tend to have thinner corneal regions, is not a significant factor in retinal damage. The visible wavelengths considered in this project did not significantly influence the heating of the fovea.

The FDA has clear guidelines regarding laser power and as shown by the model in this paper these are justified as power is a clear indicator of danger and high powered lasers should be handled with caution. However, as shown in this project, the laser diameter, or waist, is also an important factor in laser safety and should be considered more carefully when designing or distributing laser devices.

2 Introduction

Lasers come in all shapes and sizes, from high powered lasers used in research and light shows to weaker lasers used in for instance disk reading, and we all know the handheld laser or laser pointer. Used by kids, professors or cat owners they are often regarded as useful, fun and safe, with only a caveat not to point into someone's eyes. Even so, the vast majority of laser pointers are FDA safe and therefore not much thought is given to their use. Unfortunately these guidelines are not followed to the extent they should and as such ocular injuries still occur., sôметimes resulting in permanent vision impairment.

Due to the variation in production and labeling of lasers and the magnifying lens behavior of the eye, which focuses the light as per function on the fovea as seen in Fig. 1, which is known to contribute massively to vision and the high optical absorbance of the retina and the fact there is little shielding by other components of the eye makes the fovea prone to heating. Due to this heating the delicate structure of the retina can be disrupted, which can lead to eye injuries. There are cases of severe retinal damage following from what was assumed to be a harmless laser [6].

Visible light lasers such as laser pointers primarily heat the retina and pass through other parts of the eye. Although the data surrounding the transmission of light to the retina based on wavelength varies based on several studies. A general consensus is that between 85% and 95% of light within the visible spectrum reaches the retina [10, 3]. The radiant energy absorbed by eye tissue causes local tissue to heat-up, which can lead to protein degradation, loss of cell integrity, and secondary inflammatory reactions [2]. Retinal pigment epithelium contains large amounts of melanin, which works as a light absorber under physiological conditions and is also the largest absorber of energy in laser exposure. As such, the retinal pigment epithelium is the site of greatest damage when exposed to lasers.

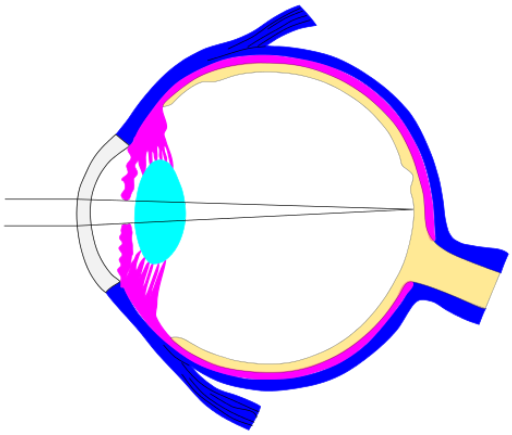

Fig. 1: Schematic of light focusing eye. A simple schematic showing how light is convexed through the lens. This refraction of laser light in the visible (400 - 760 nm) and near infrared (760 - 1400 nm) spectrum focuses the light on the focal point on the retina, the fovea[3]. Artwork from wikimedia commons.

According to the FDA [appendix C], lasers can be classified into 2 (0 - 1mW), 3R (1 - 5mW), 3B (5 - 500mW) and 4 (500+ mW). Where classification 2 and 3R are regarded as low to no eye injury hazards. 3B as medium to high and class 4, often referred to as military lasers, are severely dangerous to the human eye [6]. The lasers, which can be regarded as quasi-parallels light rays [1], depend on numerous factors such as wavelength, radiation power, exposure time, localization, and spot size. Laser pointers can cause extensive photothermal injury to the eye, because of the increase in temperature by the irradiation. There are multiple ways irradiation can affect tissue, photochemical; via interaction between tissue and the light, thermal; via interaction between the tissue and the heat originating from the light. When thermocoagulation takes place, proteins are denatured and cell death is caused. And the final phenomenon, the so-called *Hollywood laser* where tissue is destroyed or evaporated due to the extreme heat of the laser. We will disregard the latter during this project as the subject would go completely blind or worse, and disregard the first as these interactions are poorly understood. The eye has natural mechanisms against intense light flashes such as the blink reflex causing the eye to shut, preventing damage. However, this reflex has a lag time of about 0.25s. This works as a protective mechanism against injury caused by devices with a radiation output of less than 1 mW, but higher output or longer exposure can still cause injury. It is seen that in humans, thermocoagulation could be induced at an exposure time of less than 10 s and a power of 5 mW or at a higher output and shorter exposure time [2].

2.1 Problem Statement

The objective of this study is to gain a better understanding of the damage to the fovea on the retina by laser radiation within the visible light spectrum. The project aims to shed light on the influence different colored laser pointers have on eye damage as well as further subdivide the 3B type laser for these wavelengths. As shown in Shenoy et al 2015 [8] and Norren et al 2016 [9] an increase of 10°C is enough to cause protein denaturation and permanent vision loss. A blue-green (450 nm to 532 nm) laser of class 3R can cause permanent vision damage in 5 to 10 seconds [8, 9]. It stands to reason that higher powered lasers of this same wavelength will cause vision impairment in a shorter time period. In this paper we will assess the risk of laser damage to the retina for 650 nm lasers, the most common laser pointer color within the visible spectrum.

Most of the radiation from Visible (400 - 760 nm) and Near Infrared (760 - 1400 nm) wavelengths are directly transmitted to the retina [3]. This paper aims to assess the risk of common laser pointers at various parameters, including laser power, beam radius, time under irradiation, and wavelength.

To gain a better understanding of the thermal coagulation process a 2 dimensional model is designed in COMSOL Multiphysics. The model will focus on the heating of the retina during exposure to irradiation in the visible spectrum with lasers of classes 2, 2R and 3B (0 - 500mW).

2.2 Design Objectives

- Develop a heat transfer and laser light transport model for damages done by handheld laser pointers on the human eyeball which can cause retinal damage and irreversible visual impairment to the human eye. Model will acquire a realistic geometry of the human eye focused with laser pointers in visible and near infrared wavelengths.
- Understand how different aspects of time and temperature are responsible for tissue damage in the human eyeball consisting of cornea, lens, vitreous humor, retina, choroid and sclera.
- Develop a tool to help laser pointer manufacturers with various combinations of laser power and beam waist diameter, which will be within the guidelines of the FDA.

3 Methods

3.1 Schematic

The laser enters the eye via the cornea, through the aqueous humor, the pupil and lens and finally into the vitreous humor. Since we are considering the light in the visible light region, it is focused on the fovea on the retina (Fig. 1.). Here the vitreous humor acts as the required distance required to focus the light. Some light gets scattered and absorbed during the path it takes before reaching the retina. Beyond the retina are the choroid and sclera, which serve to supply blood and provide structural support, respectively.

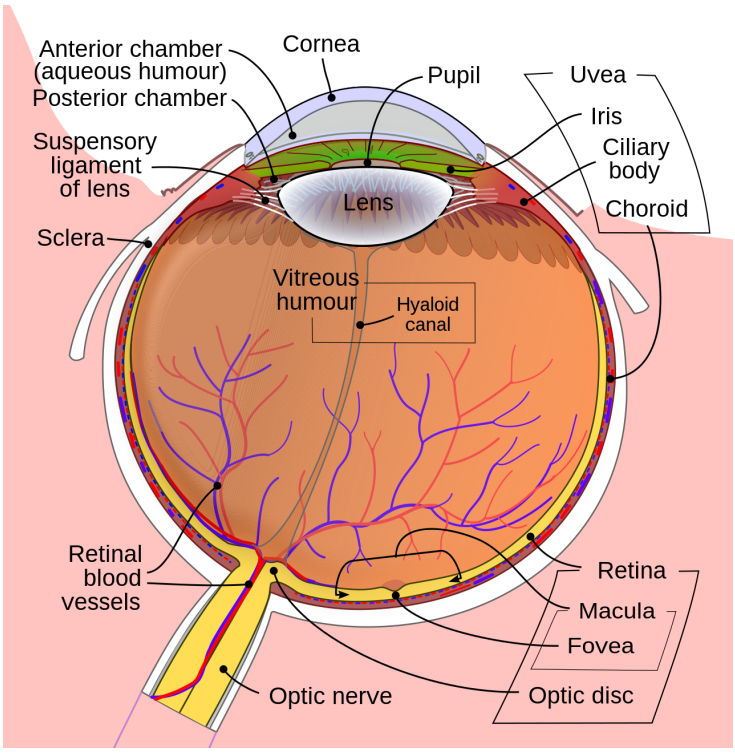

Fig. 2: Schematic of human eyeball. A detailed view showing all layers in the eyeball. The lens, aqueous humor and iris / pupil are regarded as one domain within the COMSOL approximation due to their physiological similarities and little effect on conductive and convective heating. Artwork from wikimedia commons.

To study damage done to the retina via laser irradiation, the eye is approximated into a COMSOL geometry. Where the aqueous humor and lens (Fig. 2.) are combined into a front eye component (Fig. 3.). This is justified as the heating of these elements likely only contributes slightly to the heating of the retina through conductive and convective heating. The majority of heat generation comes from the point of contact of the laser with the retina.The majority of laser light will be transmitted through the non-retinal components and will be absorbed by the retina [10].

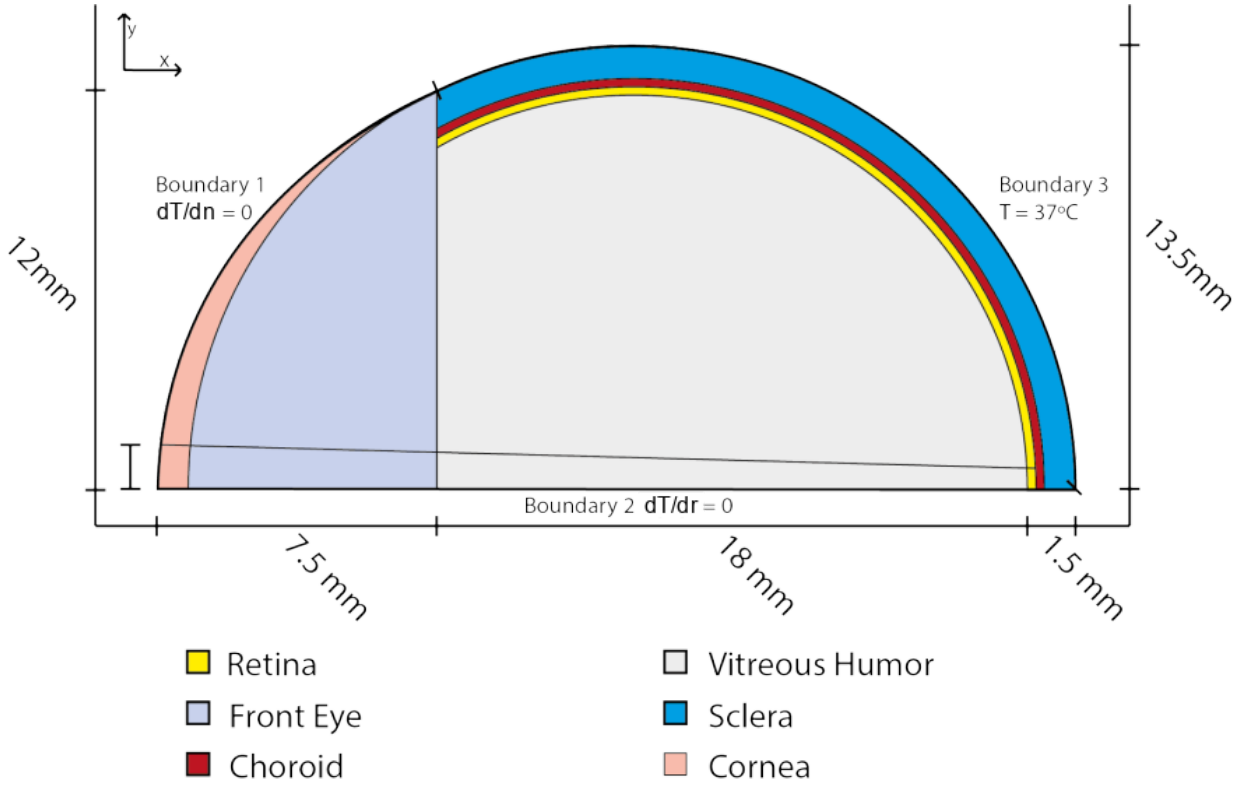

Fig. 3: COMSOL model schematic. 2D Axisymmetric view of our model of the human eye. Indicated with the diagonal line is the laser domain which is dependent on incoming laser radius and fovea width (smaller domain in Cornea and Retina, respectively). Cornea, Retina, Choroid and Sclera are regarded as variable among people. Measurements are not precise and are seen as indicating only. **Note:** The sclera and choroid vary in thickness. For simplicity, we regard the choroid as having a thickness of 250 microns, and the sclera having a thickness of 1 mm.

3.2 Governing Equations

The two major equations of heat transport in the eyeball and laser transport in the eyeball will be applied to all regions / surfaces as per the schematic.

Heat transfer in all regions of the eyeball is given by the equation [4]:

$$\rho c_p \left(\frac{\partial T}{\partial t}\right) = \frac{1}{r}\frac{\partial}{\partial r}\left(k.r\frac{\partial T}{\partial r}\right) + \frac{\partial}{\partial z}\left(k\frac{\partial T}{\partial z}\right) + Q \qquad \text{(Eq. 1)}$$

The term dropped from the heat transfer equation is the convection term. We dropped this term since there is no bulk fluid motion/flow in our geometry.

Laser Irradiance is given by the equation [21]:

$$I(r, z, t) = I_0 \exp\left(-\frac{2r^2}{w^2} - \alpha z\right) \exp\left(-\frac{8t^2}{\tau^2}\right) \qquad \text{(Eq. 2)}$$

where, I_0 is the incident value of intensity [W/m^2]
w is the beam waist [mm]
τ is the laser pulse duration [ms]
r is the radius of the beam [mm]
α is absorption coefficient [1/m]
z is the length of the model [mm]
t is the time taken for the laser to travel [sec]

The pulses for the laser are characterized by the function: $exp(-\frac{8t^2}{\tau^2})$. This returns a decreasing exponential laser pulse.

For a given laser parameter, the laser intensity at the cornea is calculated from [21]:

$$I_c = \frac{4P}{d_c^2 \pi} \qquad \text{(Eq. 3)}$$

where, P is the laser power [mW]
d_c is the beam diameter on the cornea [mm]

Diameter of the image and intensity on the retina is given by the equation [21]:

$$d_r = 2.4\frac{\lambda f}{d_p} \quad \text{(Eq. 4)}$$

and

$$I_r = I_c \frac{d_p^{\,2}}{d_r^{\,2}} \quad \text{(Eq. 5)}$$

where, λ is the laser wavelength [nm]
f is the focal distance of the lens [mm]
d_p is the diameter of pupil opening [mm]

Heat Source due to Laser [21]:

$$Q(r, z, t) = \mu_a \, I(r, z, t) \quad \text{(Eq. 6)}$$

where α is the wavelength-dependent absorption coefficient of the specific tissue [1/m]

3.3 Initial Conditions

$$T|_{\text{boundary 1}} = T|_{\text{body}} \quad \text{(Eq. 7)}$$

3.4 Boundary Conditions

$$T|_{\text{boundary 3}} = 37°C, \text{ at all t} \quad \text{(Eq. 8)}$$

$$\frac{dT}{dr}|_{\text{boundary 2}} = 0, \text{ due to axi-symmetry} \quad \text{(Eq. 9)}$$

$$\frac{dT}{dn}|_{\text{boundary 1}} = 0, \text{ where } n \text{ is the normal direction to boundary 1} \quad \text{(Eq. 10)}$$

Boundary condition at back of retina:

Heat regulation throughout the body is predominantly affected by blood flow, keeping tissue at a constant temperature of approximately 37°C. Within the eye the choroid, a layer behind the retina consisting of many blood vessels, is responsible for this thermal regulation [11].

3.5 Assumptions

1. The aqueous humor, iris and lens are combined as the "front eye".
2. The Fourier heat equation can be used as the governing energy equation only if the eye is considered as containing only solid or stagnant fluid.
3. Laser light travels directly through the center of the eye, passing only through the cornea, lens, aqueous humor, vitreous humor, and retina.
4. The laser is held at a constant point for a given period of time.
5. The optical nerve is disregarded in the symmetry of the geometry.
6. Light will not penetrate past the retina because of high absorption coefficient values.
7. Light is perfectly collimated and beam radius does not change over a short distance.

3.6 Parameters

Absorbance Coefficients

Ocular media absorbance coefficients were determined from values measured from ocular media of Rhesus monkeys [23]. The absorbance coefficients that were incorporated into this model are the cornea, lens, and vitreous humor.

Retinal absorbance coefficients were determined using the function derived from Jacques et. al [29], where he estimates the absorbance coefficient of the retina to be as seen in Fig. 4.

$$\mu_a(\lambda\,[nm]) \approx 6.49 * 10^{12}\,\lambda^{-3.48}\ [1/\text{cm}]$$

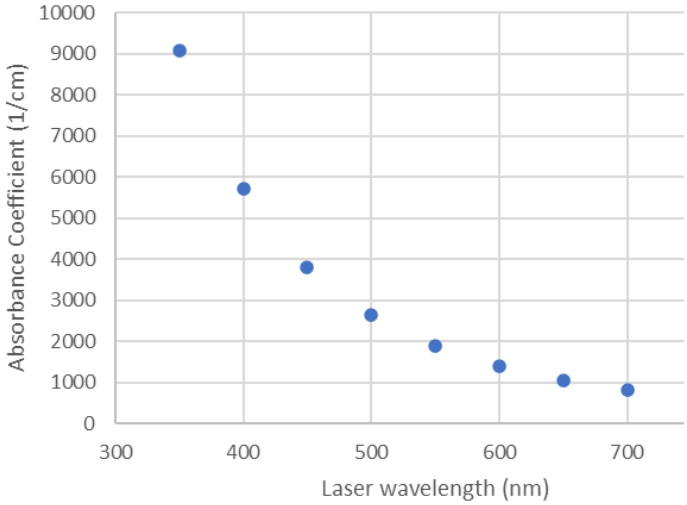

Fig. 4: Retinal absorbance coefficients in the visible spectrum. This graph shows the correlation between the absorbance coefficient μ_a [1/cm]. Although different values are available online, as discussed in Fig. 16, these values are used in the COMSOL model for the standard runs. Equation from: [28, 29]

4 Results and Discussion

4.1 Geometric Model

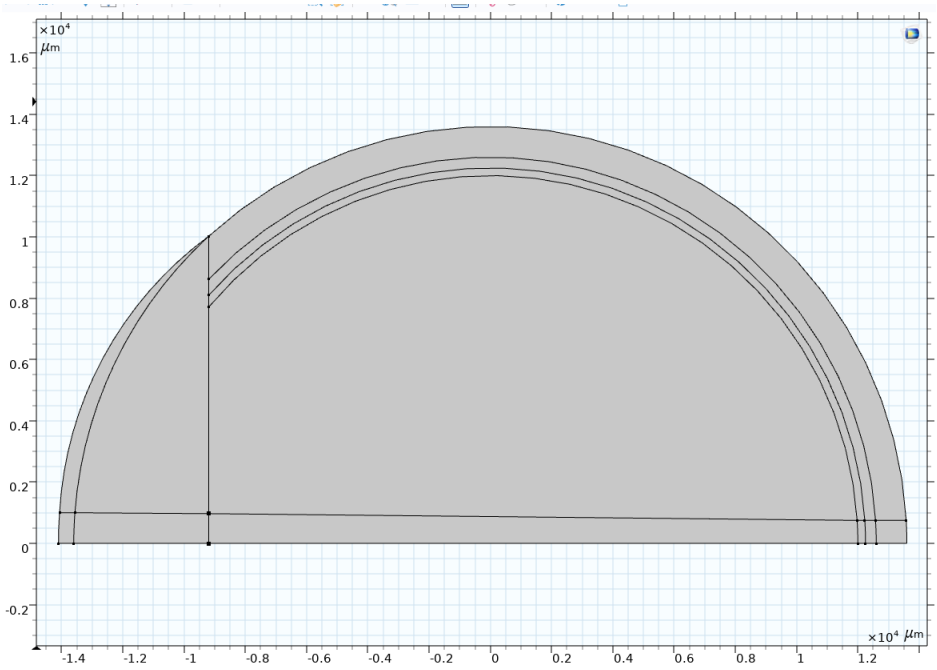

Fig. 5: COMSOL model of the eye. This 2D Axisymmetric COMSOL model of human eye includes the cornea, front eye (lens, iris and aqueous humor), vitreous humor, retina, sclera, and choroid (as shown in Fig. 3) in the correct dimensions as denoted in the model.

This model assumes conductive heat transfer occurs throughout all of the components of the eye, with a temperature boundary condition at the back of the sclera at 37°C. It also assumes that the light equation only applies to the cornea, front eye, vitreous humor, and retina. This is because of assumption 6, that no light penetrates the back of the retina, due to its very high absorbance in visible wavelengths.

The interior section of the eye represents the path of laser light taken. It assumes that the light is focused to converge at the fovea, a section of the retina with a radius of 0.75 mm. The angle that the light converges to depends on the laser beam radius.

4.2 Temperature Surface Plot

The computational model shows a temperature increase over a period of 10 seconds due to irradiation by a red type 3R laser. Fig. 6 indicates localisation of this heating is primarily on the surface of the foveal region of the retina. Fig. 7 shows how the temperature at the center of the fovea increases over time where it reaches an increase of 7.5°C after 8 seconds then levels off.

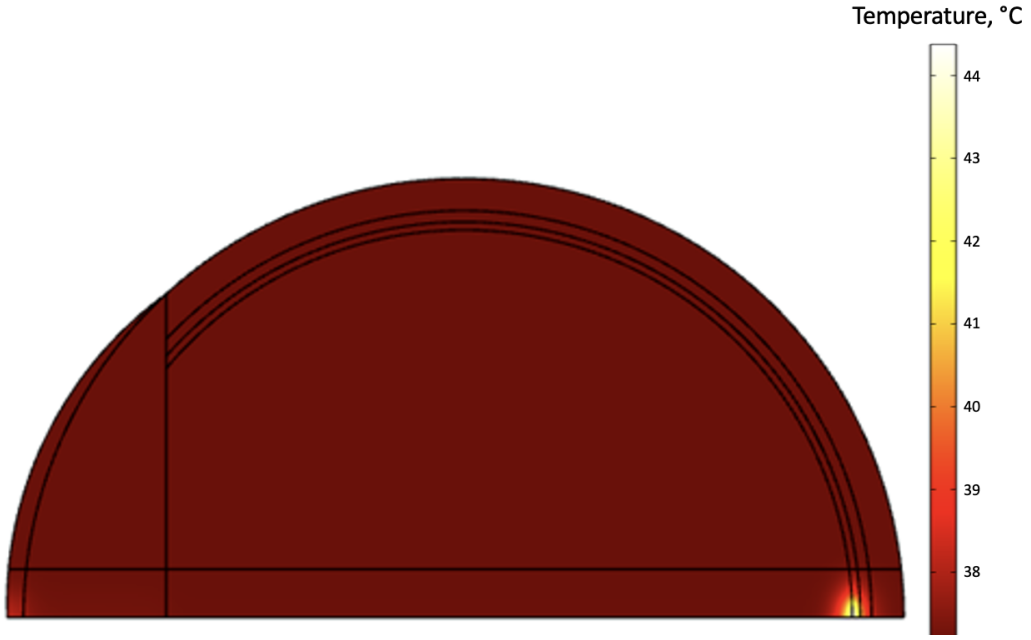

Fig. 6: COMSOL surface plot. Temperature Surface Plot after 10 seconds with laser parameters 5mW, 650 nm and 50 µm beam radius laser focused directly on the center of the retina for 10 seconds. Notably the heating occurs predominantly in the center of the retina (fovea), where a temperature increase of around 7.5°C is observed. This is due to the low absorption of light in the prior components, therefore the majority of the laser power is absorbed on the retina, which has a relatively high absorption coefficient for this wavelength.

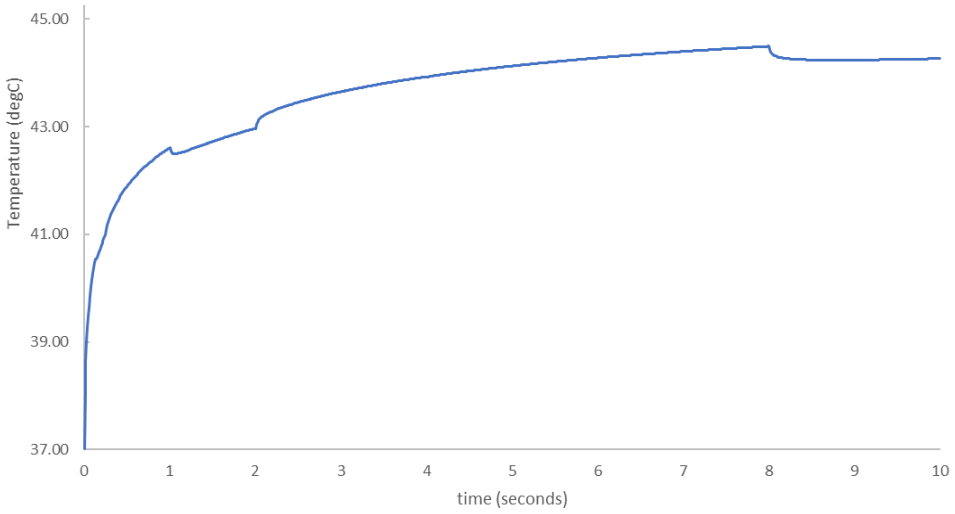

Fig. 7: Temperature graph over time. Temperature Over Time Plot of the center of the foveal surface with laser parameters 5mW, 650 nm and 50 µm beam radius laser focused directly on the center of the retina for 10 seconds. The plot shows the temperature increases rapidly for the first second, after which it levels off. The plateauing behavior might be caused by the neighboring choroid transporting heat out of the system. During this computation a temperature increase of 7.5°C is reached after 8 seconds.

4.3 Mesh Convergence: Global

During initial global mesh convergence, a parametric sweep was performed of 8 mesh sizes (Table 1.) for the temperature of the fovea after 10 seconds. The fovea temperature converges after extra fine mesh, indicating that extra fine is the appropriate mesh size. Fig. 8 shows the convergence of final temperatures given different mesh sizes in Absolute Relative Error. Fig. 9 shows the constructed mesh at "extra fine" mesh size.

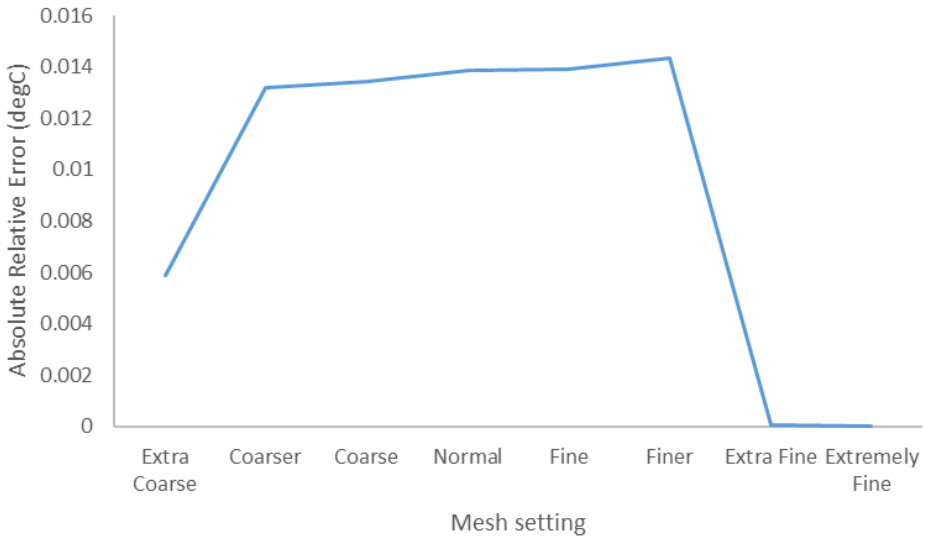

Fig. 8: Global Mesh Convergence. This plot shows the Absolute Relative Error of 8 different global mesh configurations. This error converges when settings are "extra fine" and "extremely fine" indicating convergence. However, at all levels of mesh size, the error remains extremely low, within 0.015°C.

Table 1: Mesh convergence mesh sizes. This table shows the mesh size specifics used in global mesh convergence.

Parameter	Extra Coarse	Coarser	Coarse	Normal	Fine	Finer	Extra Fine	Extremely Fine
Max element size	5540	3600	2770	1860	1470	1020	554	277
Min element size	443	166	55.4	8.31	8.31	3.46	2.08	0.554
Growth Rate	1.8	1.5	1.4	1.3	1.3	1.25	1.2	1.1
Curve Factor	0.8	0.6	0.4	0.3	0.3	0.25	0.25	0.2

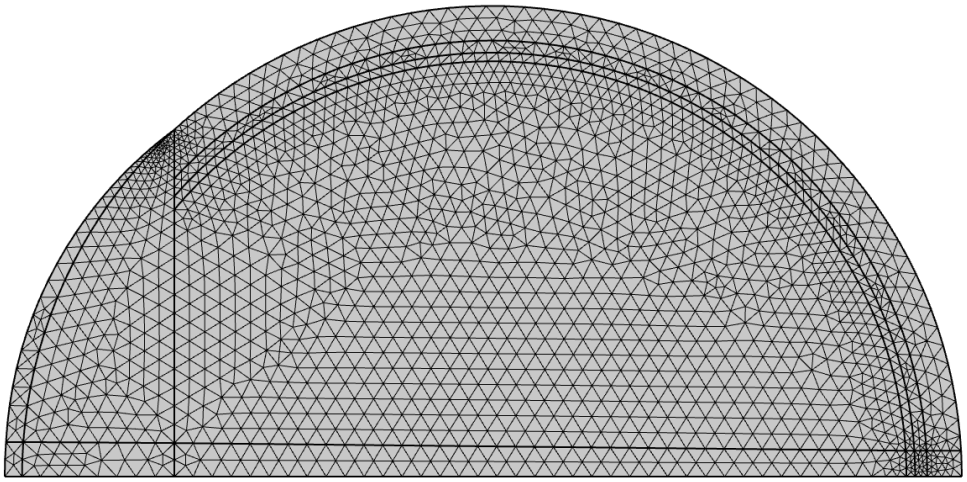

Fig. 9: Global Mesh Geometry. This figure shows a free triangular mesh model of the human eye under extra fine mesh parameters (Table 1.). The model converges per temperature of the fovea after 10 seconds as shown in Fig. 8.

4.4 Mesh Convergence: Inner Model

Further analysis shows that the section of the model that affects the solution most heavily is the area closest to the axis of symmetry. This section is where the laser passes through, therefore a significantly finer mesh is required for the innermost section of the model. The bottom 1.5 cm of the model has been partitioned into a section with different mesh settings than the rest of the model.

A mesh convergence analysis was conducted with 0.01 seconds of heating of a 5 mW, 50 µm beam radius, 1 ms pulse duration, 650 nm laser. The results of the parametric sweep showed that our solutions converge when using a maximum element size of 80 and a minimum element size of 0.1 only for the fine mesh domains. Fig. 12 shows the final mesh of the computational model.

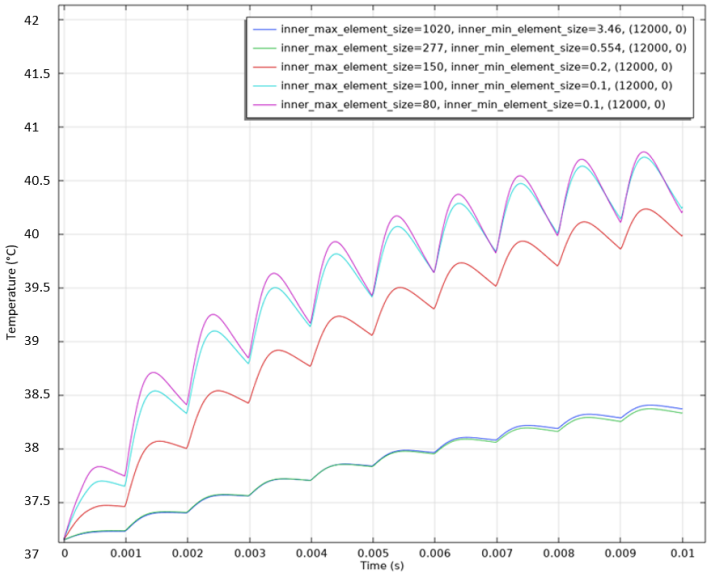

Fig. 10: Temperature Plots of Parametric Sweep. Temperature Over Time Plot of the center of the fovea with laser parameters 5mW, 650 nm and 50 µm beam radius laser focused directly on the center of the retina for 0.01 seconds. The oscillation seen for each mesh setting is caused by each 1 ms pulse. Legends on the top right indicate the maximum and minimum element size.

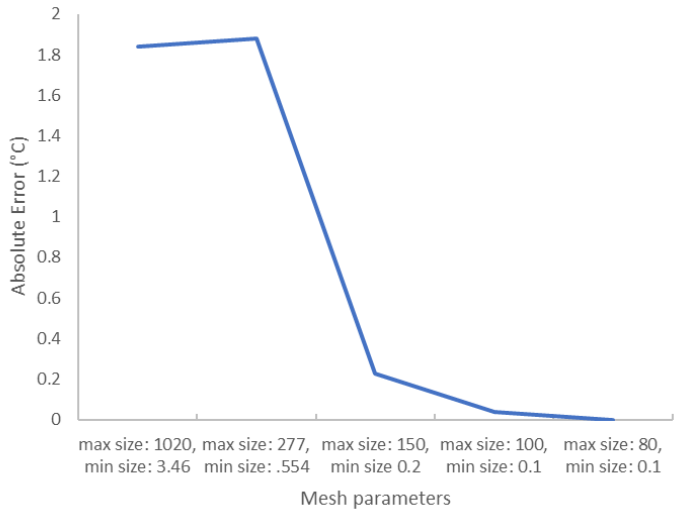

Fig. 11: Inner Mesh Convergence. This plot shows the Absolute Relative Error of 8 different global mesh configurations.

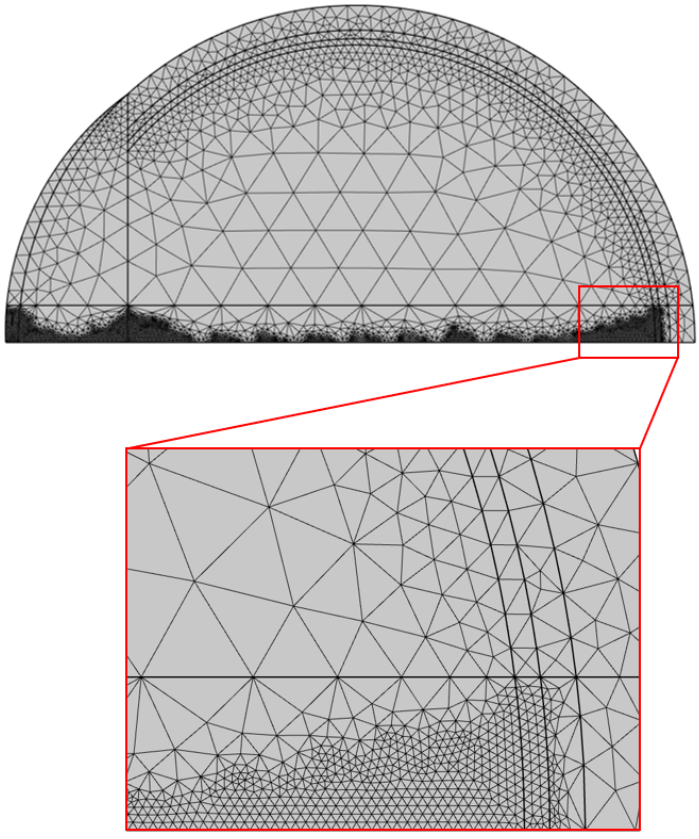

Fig. 12: Final Mesh. This figure shows a free triangular mesh model of the human eye under mesh parameters max_size: 80 and min_size: 0.1. There are significantly more mesh elements along the laser irradiance path.

4.5 Time Step Convergence

A convergence analysis was conducted for time stepping. The time steps were determined to be a function of pulse duration. Therefore, for a 1 ms laser, the time step must be less than 1 ms in order to capture the waveform of the laser pulses within the computation. Data for a parametric sweep was conducted as seen in Fig. 13, for a 650 nm, 5 mW laser with 50 um beam radius and 1 ms pulse duration for a 0.1 second heating duration. Solutions converged after 0.02*laser pulse duration, or 0.02 ms time stepping (Fig. 14).

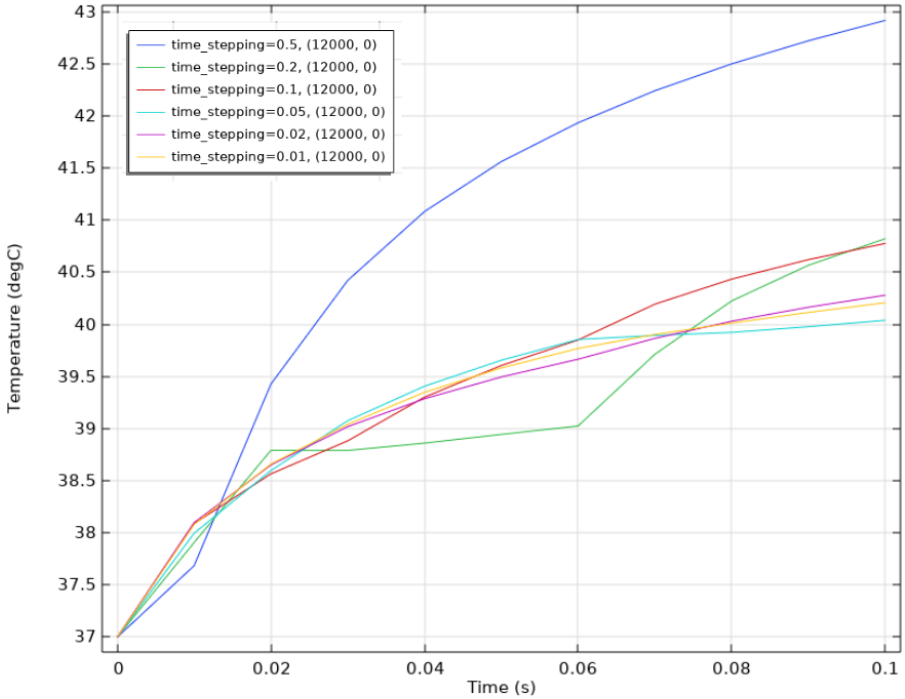

Fig. 13: Time stepping parametric sweep. The figure shows that time stepping has a large influence on final temperature. The shape of laser pulses changes rapidly and as a result, is sensitive to sampling frequency. Data collected for a 650 nm, 5 mW laser with 50 um beam radius and 1 ms pulse duration for 0.1 seconds.

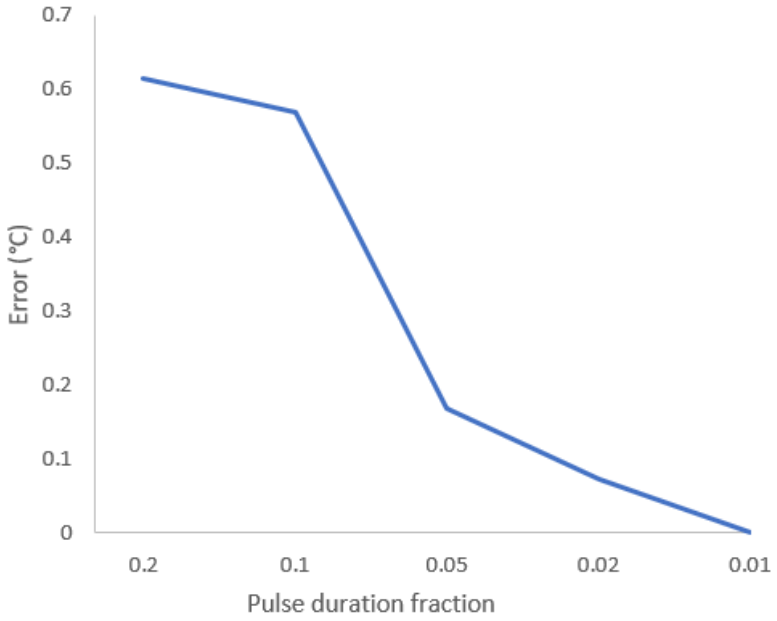

Fig. 14: Time Step Error convergence. This plot shows the Absolute Relative Error in degrees Celsius (°C) of 5 different pulse duration fraction configurations. The error diminishes as pulse duration fraction decreases, requiring more time steps per second.

4.6 Model Validation

4.6.1 Results Validation

Our solution predicts a peak temperature increase of 7.5°C after 8 seconds and an overall temperature increase of 7.3°C after 10 seconds of heating. This data was gathered from a computed solution using a 5 mW, 650 nm, 50 µm beam radius laser focused on the fovea over 10 seconds. A case study of laser retinal damage was reported [24] which states that a patient received retinal injury after 10 seconds of direct heating into the eye with a laser with 5 mW, 635 nm, and a 50 µm beam radius. This case study reports a retinal temperature increase of 6°C to 10°C, which falls within the bounds of the computed solution. Both the computed solution and the case study involve a 5 mW, 50 µm beam radius laser. The differences between the two lasers are the wavelengths (635 nm and 650 nm) and the pulse durations, which were unreported in the case study.

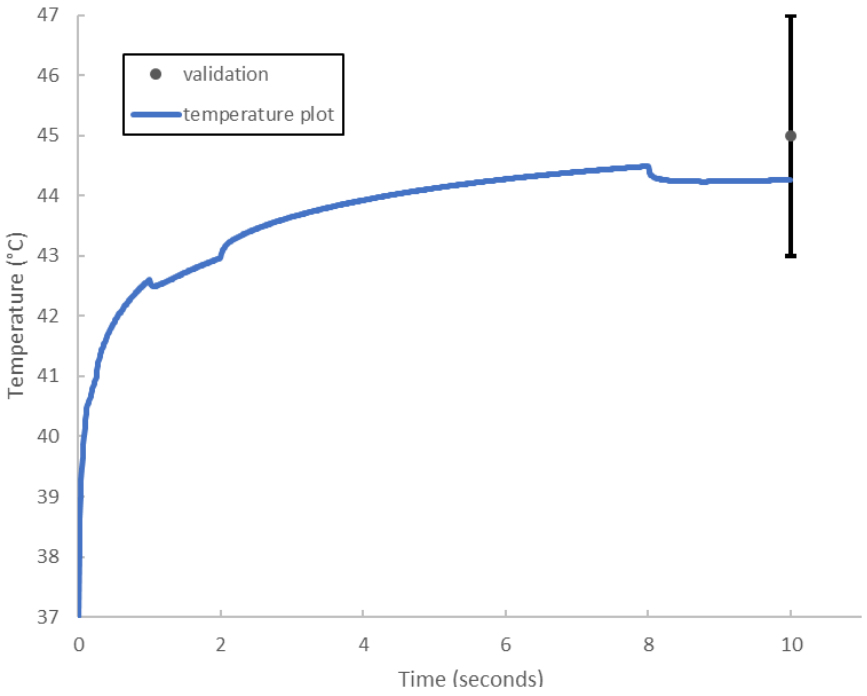

Fig. 15: Validation against literature data showing computed temperature at the end of 10 seconds is within the range of temperature increase for a similar laser causing retinal injury. Computational model calculated from 10 seconds heating 5mW laser 650 nm 50 µm beam radius 1 ms pulse duration.

4.6.2 Parameter Validation

Retinal absorption coefficients are inconsistently reported between researchers. Several sources report vastly different absorption coefficients at the same wavelengths. This could be due to discrepancies in melanin concentration between retinal samples. Retinal absorption is highly dependent on melanin concentration; melanin concentrations can be responsible for changes in Retinal pigment epithelium (RPE) absorbance up to four times in certain wavelengths [32].

The retinal absorption coefficients implemented in the computational model, from Jacques, et al. [28] are validated against several other reports of wavelength dependent retinal absorption coefficients [30, 32, 33]. As shown in Fig. 16, the values used from Jacques et al. seem to fit reasonably with other reports. In Section 4.7.4 and 4.7.5 of this report, the effect of variation in retinal absorption coefficients is addressed.

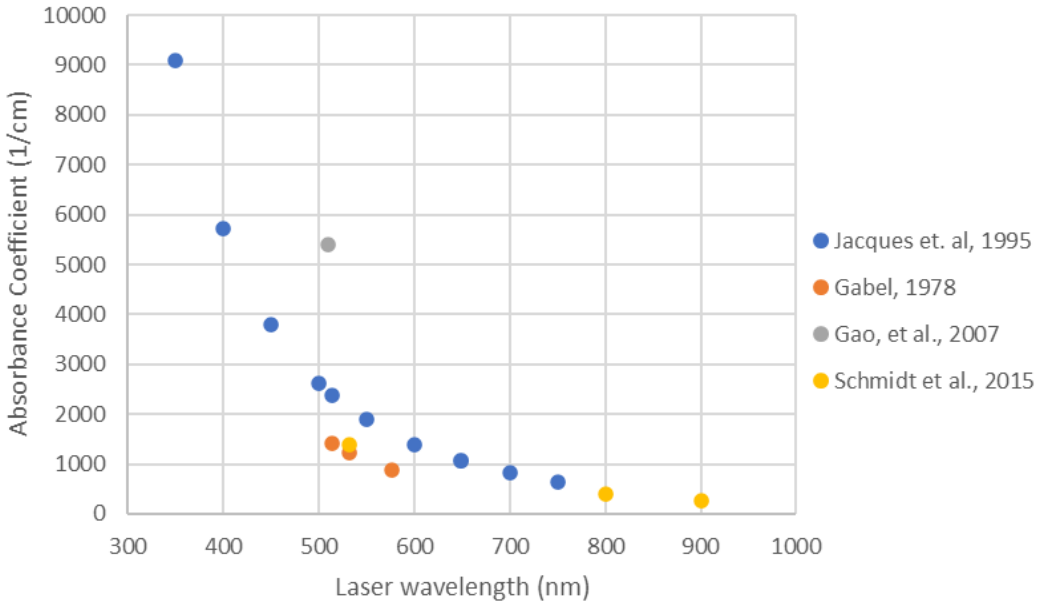

Fig. 16: Retinal absorption coefficients at different wavelengths. This figure indicates measurements for absorption coefficients μ_a [1/cm] fluctuate in literature. These values are used as range indications for parameter validation and variation. As denoted in Fig. 4. The data from Jacques et al 1995 are used throughout the COMSOL model if not denoted otherwise.

4.7 Sensitivity Analysis

In Sensitivity Analysis, various parameters are investigated on the degree of impact on the temperature of the retina after laser heating. Corneal thickness, laser power, laser beam waist, and retinal absorbance coefficient are the parameters that are studied. In each section, a parametric sweep was completed through COMSOL that computed the temperatures of the eye after 1 second of laser heating. These parameters were chosen since they appear to have a significant effect on final retinal temperatures, and they are parameters that are often variables in laser heating of the human eye.

4.7.1 Corneal Thickness

Cornea thickness varies among individuals, ranging between 470 to 630 microns [22]. Corneal thickness is investigated as a factor in laser retinal damage through a sensitivity analysis. The cornea is the first boundary in which the laser passes through the eye. Compared to other ocular media excluding the retina, the cornea tends to have the highest absorbance coefficient [23]. Therefore, the cornea plays a role in diminishing the irradiance of an incoming laser before it reaches the retina.

The computation for the sensitivity analysis is based on laser heating of 1 second from a 5 mW, 650 nm, 50 μm beam waist, 1 ms pulse laser. Corneal thickness is related to final temperature after 1 second of heating through a negative linear function given by:

$$T@t=1sec\ (x\ [\mu m]) = -0.00013x + 47.137,$$

where x is corneal thickness in μm (Fig. 18). This result is expected, since an increase in corneal thickness will decrease the irradiance that reaches the retina, reducing retinal heating.

There is an insignificant effect of corneal thickness on the final temperature of the retina. Between individuals with thick corneas and those with thin corneas, the final temperature increase after 1 second of laser heating is increased by only 1.4%, which equates to a difference of 0.13°C.

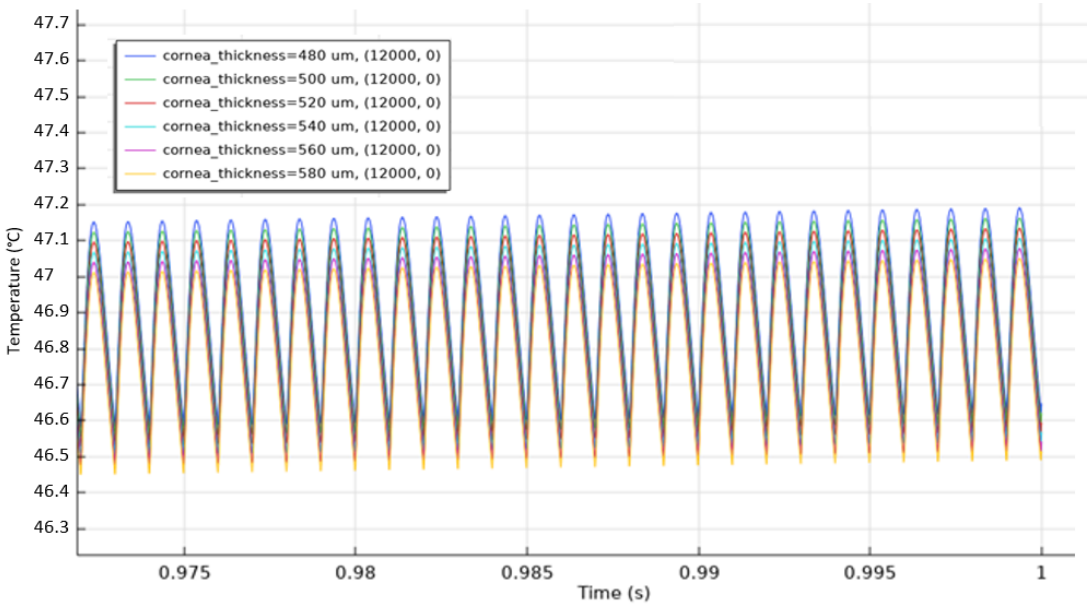

Fig. 17: Foveal Surface Temperature of multiple corneal thickness. This figure indicates the (minor) effect cornea thickness has between the physiological range 480 micrometer to 580 micrometer. Parameters used are 5 mW, 650 nm, 50 µm beam waist and 1 ms pulse duration.

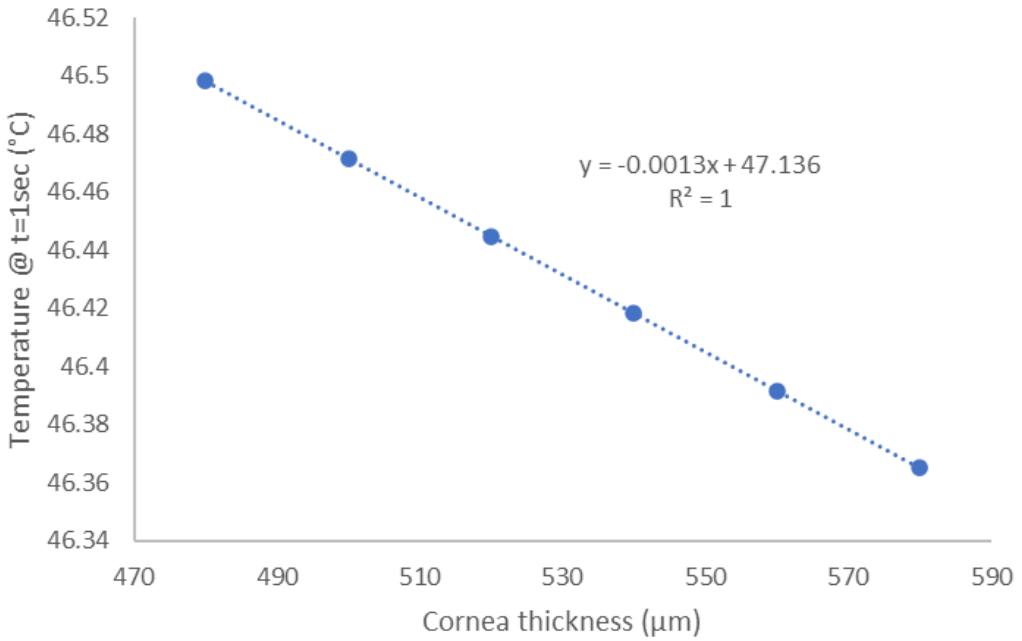

Fig. 18: Final temperature of the foveal surface for different corneal thickness. As indicated in Fig. 17. The effect of cornea thickness plays a minor role in preventing the irradiation from reaching the fovea, as such the difference in final temperature between 480 and 580 um changes an insignificant amount.

4.7.2 Laser Power

Laser power was investigated as a factor on the final retinal surface temperature given identical laser parameters (650 nm, 50 µm beam waist). Laser power was tested at 5 mW, 20 mW, 50 mW, and 100 mW (Fig. 19). Laser power also relates to final temperature as a linear function *(Fig. 20)*, given as:

$$T@t=1sec\ (x\ [mW]) = 1.8943x+37,$$

where x is laser power in mW.

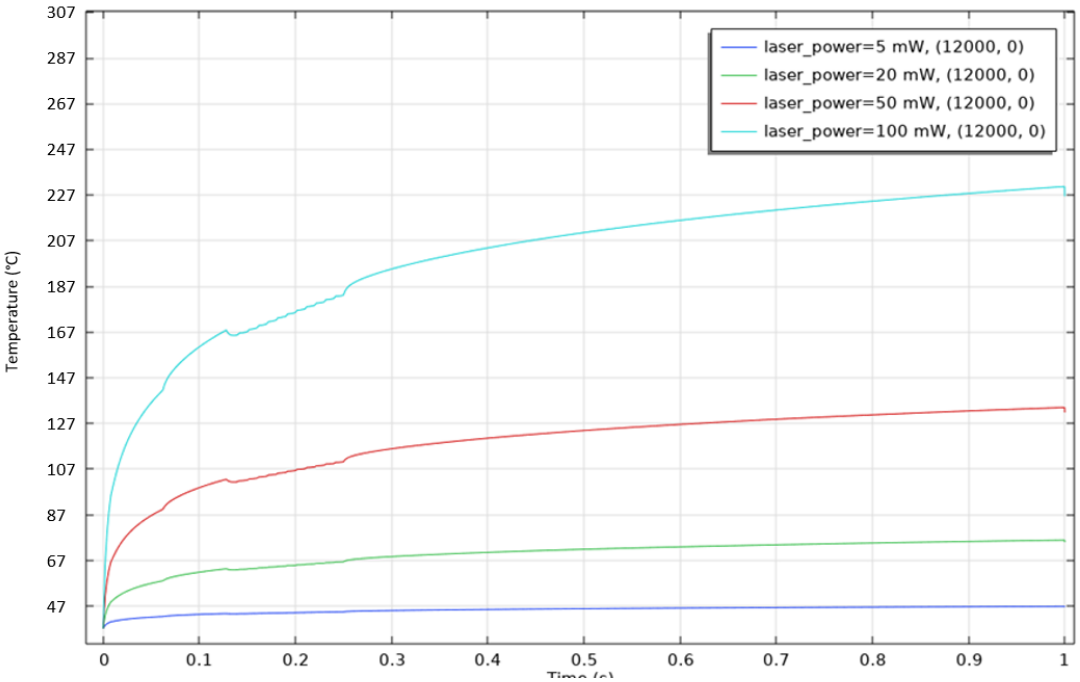

Fig. 19: Foveal Temperature of the foveal surface for different laser powers. This figure shows how the temperature of the fovea after 1 second is influenced by laser power. Ranging between from 5mW to 100mW, where severe heating of the fovea occurs. This is directly linked to vision impairment. Parameters used are 650 nm, 50 µm beam waist and 1 ms pulse duration.

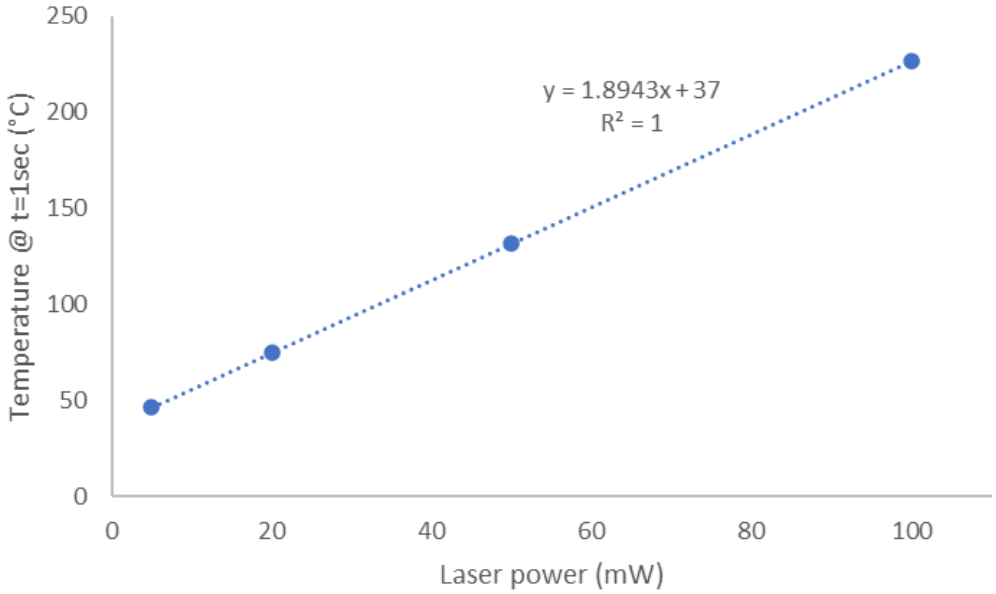

Fig. 20: Final temperature of the foveal surface for different laser powers. This image similarly to Fig. 19 shows a massive increase in final temperature of the fovea after heating for 1 second using red lasers with powers ranging from 5 to 100 mW. It shows a linear correlation which allows us to calculate a power around 6mW would be enough to cause photothermal burns on the fovea after 1 second.

4.7.3 Beam Waist

Beam waist is defined as the radius of the location where irradiance is at least 13.5% of the maximum value [27] (Fig. 21). Since we are assuming a perfectly collimated laser from a short distance, it can be assumed that the beam waist stays constant throughout the laser's path. Having a smaller beam waist focuses the light on a smaller point, increasing the irradiance and heating at that point.

In Fig. 22, temperature plots for 5 different beam waists are shown: 30, 40, 50, 60, 70, 80, and 90 μm. The peak temperatures on the retina surface increases as beam waist decreases, and overall temperature increases throughout the retina when the laser is more focused (Fig. 23(a,b,c)). This result is expected, since a higher focused beam will result in a higher peak retinal temperature.

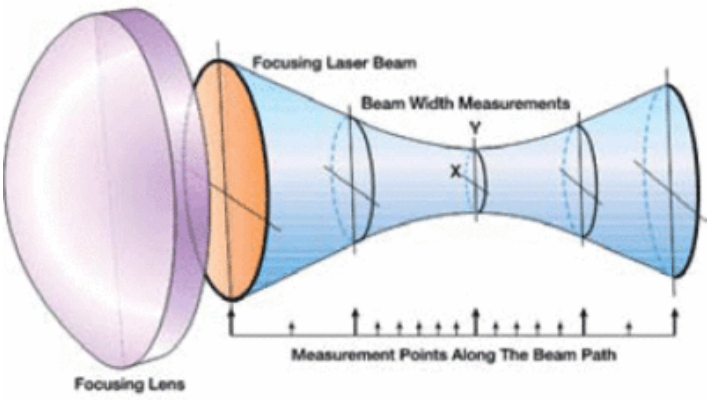

Fig. 21: Illustration of a laser's beam waist. Image shows relative intensity is distributed over the radial position where W denotes laser radius. Image from: wikimedia commons.

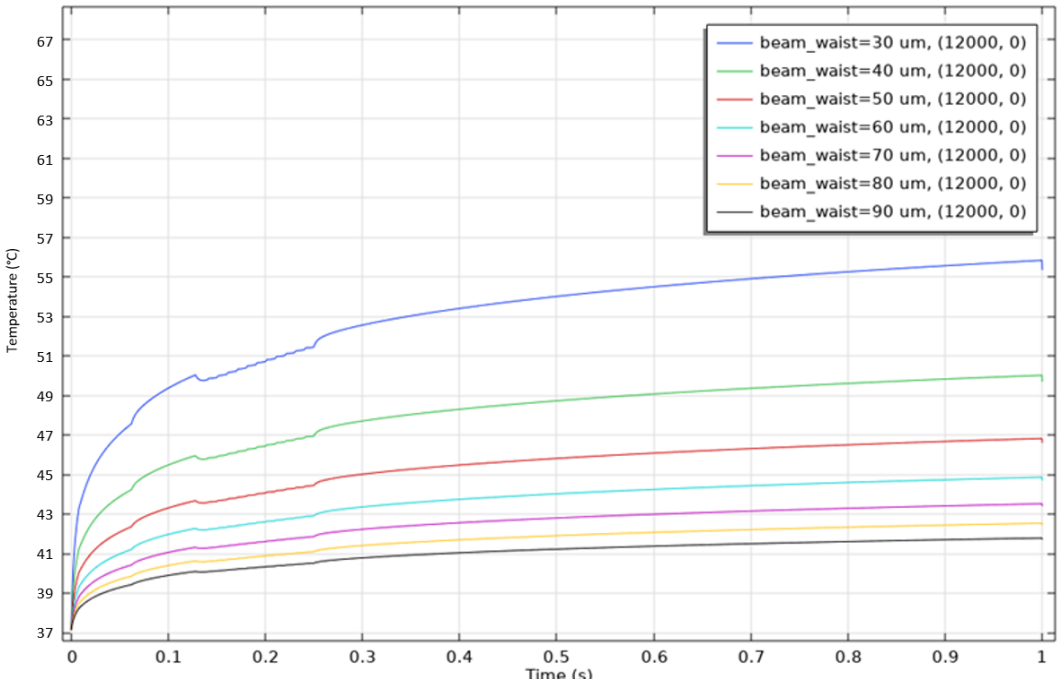

Fig. 22: Foveal Temperature Plots of heating given different beam radii. Image shows beam waist influences the heating of the fovea significantly where a broader laser heats the fovea less relative to a more narrow or condensed ray. Parameters used are 5 mW, 650 nm and 1 ms pulse duration over a period of 1 second.

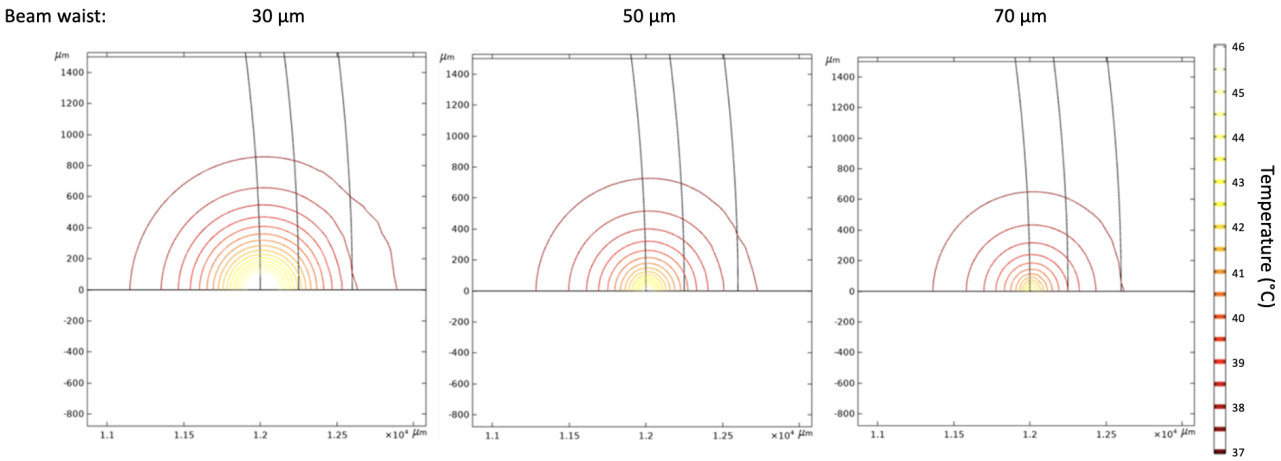

Fig. 23: Contour plot of foveal heating. This image is a comparison of the isothermal contours of beam waist at (a) 30, (b) 50, and (c) 70 µm. The figure indicates a negative correlation between heat dissipation and beam waste. Parameters used are 5 mW, 650 nm and 1 ms pulse duration over a period of 1 second.

4.7.4 Retinal Absorbance Coefficient

Retinal absorbance coefficient determines how much irradiance is absorbed as heat into a given tissue, and it also determines the rate at which irradiance decays in a tissue. As the retinal absorbance coefficient increases, the peak temperature in the retina decreases. This result is counterintuitive, since the absorbance coefficient directly affects the heating of the retina.

However, in the retina, irradiance eventually becomes zero very rapidly due to the high absorbance coefficient. Therefore, the rate at which irradiance diminishes in the retina has a large effect on the total irradiance within the retina. Since increasing the absorption coefficient exponentially decreases irradiance, less of the retinal thickness will contribute to heating. As a result, the overall temperature of the retina decreases due to an increase in absorption coefficient (Fig.. 24).

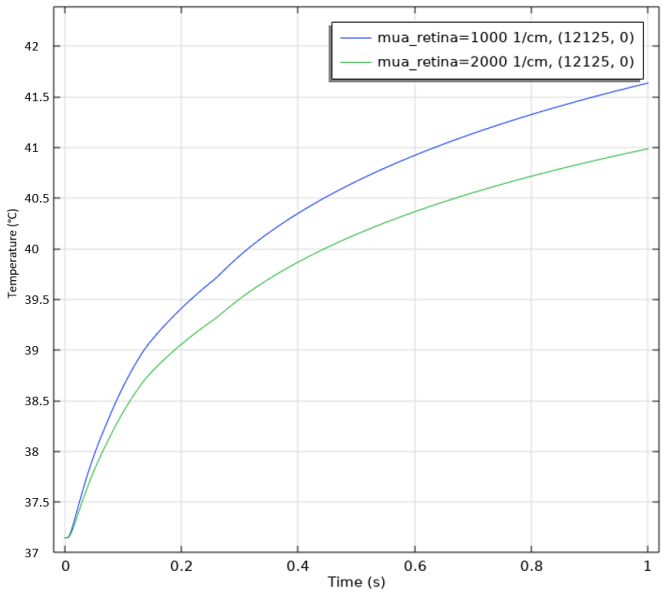

Fig. 24: Foveal Temperature Plot. Image shows the relationship between absorbance coefficient and foveal heating. Parameters used are 5 mW, 650 nm (for ocular media excluding the retina), 50 µm beam waist and 1 ms pulse duration over a period of 1 second.

4.7.5 Complete Sensitivity Analysis

All parameters tested for sensitivity were also adjusted by +10% and -10% to determine the magnitude of temperature change in the retinal surface. From the sensitivity analysis, the largest impact parameters on the computational model are beam radius and laser power (Fig. 25).

Absorbance coefficient has an extremely low effect on the final temperature change of the retina. This conclusion is unexpected, since the absorbance coefficient directly impacts the heating of the retina's heat generation term. However, laser wavelength tends to change the retinal absorbance coefficient drastically [28, 29]. While most eye parameters such as absorbance coefficients and geometry differ slightly between individuals and laser wavelengths, retinal absorbance coefficients in the visible spectrum range from less than 1000 [1/cm] to over 9000 [1/cm], depending on wavelength [28].

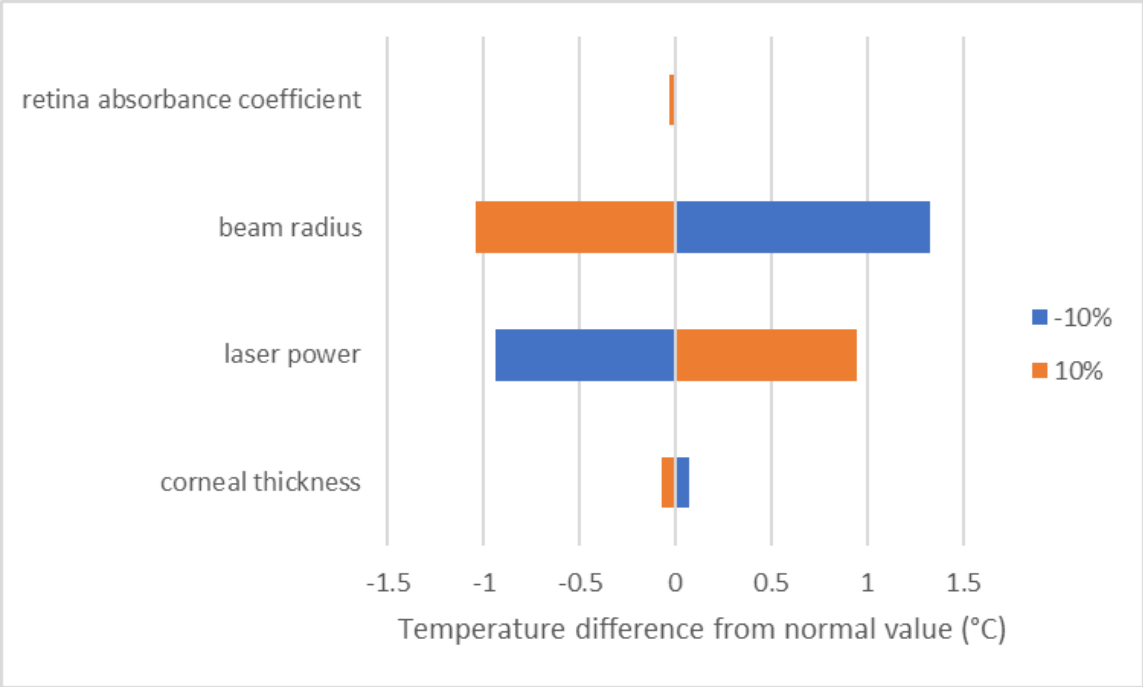

Fig. 25: Temperature differences when compared to normal parameters. Image shows temperature difference from the normal value of several key parameters when increasing or decreasing each parameter by 10%. The figure indicates beam radius and laser power are sensitive components where a negative or more narrow beam radius has a proportionally large influence compared to a wider beam.

5 Conclusions and Design Recommendations

Cornea thickness, laser power, retinal absorbance coefficient and beam waist data were altered to determine what combination of these parameters will do most damage to the retina. Mild thermal coagulation damage to the retina occurs at a minimum temperature increase of 10°C [9].

Our validation shows that our computational model accurately predicts a retinal temperature increase for a laser with 650 nm wavelength, 5mW and 50 μm beam radius. This verifies the conclusion that 5 mW laser power is safe to use under most circumstances and will not cause permanent thermal damage to the retina within reasonable time limits. Through the analysis of the results of this computational model, it is apparent that hand held laser pointers operating with a power less than or equal to 5mW within the visible spectrum are safe to use.

Safety: For our model with a laser wavelength of 650nm, laser power of 5mW and 50 μm beam radius, we observed that with a proper selection of the laser power and beam waist the laser will not damage the retina. But, if the beam width is small in diameter, the laser can cause damage to the fovea by increasing the temperature much more than that of a larger beam width. This way we can mitigate the risk of damage on the fovea by using lasers with a larger diameter of beam width. Also, one should use a lower power laser as suggested by the FDA (see Appendix C) for handheld laser pointers.

5.1 Predictive Model

In 4.7 Sensitivity Analysis, functions estimating peak retinal temperatures, dependent on laser power and beam waist, were derived. Laser power was found to be perfectly linearly correlated with peak retinal temperatures, and laser beam waist data was found to fit onto a 3rd order exponential function with a R^2 value of 0.9989. Using these estimation functions, we are able to create a predictive tool for lasers to estimate the peak temperature of the retina after 1 second of heating. This tool is shown in Fig. 26, which shows estimated final temperatures given a particular laser power and beam waist. For best results, this tool should only be used in wavelengths near 650 nm, where the solutions were calculated from.

The horizontal red line indicates the threshold for laser-induced thermocoagulation damage onto the retina. Therefore, after 1 second of heating, only those lasers above the horizontal red line indicate possible thermal coagulation damage on the retina.

From an analysis of the trend of retinal heating over time, it is clear that the majority of retinal heating occurs within the first few moments. Our computational model predicts that 65% of the total temperature increase over 1 second of heating occurs within the first 0.1 seconds, which is the time it takes for the blink reflex to prevent further laser heating. Therefore, the horizontal purple line in Fig. 26 indicates lasers that can induce thermal damage onto the retina after 0.1 seconds.

This predictive model can be a valuable tool for assessing the possible safety hazards of a particular laser, without the need for further computation or experimental data. This tool can be used by manufacturers when designing safe laser pointers and by consumers looking to assess the possible risk of a particular laser.

For manufacturers, the FDA limits the power output for laser pointers to 5 mW for lasers in the 400 to 710 nm range [25] (See Appendix C). However, there is no FDA regulation on beam radius for laser pointers. From the predictive model, it is clear that even if certain lasers have a low power output, they can still cause retinal damage if the beam radius is small enough. This is important information for manufacturers and consumers to consider when designing or purchasing laser pointers.

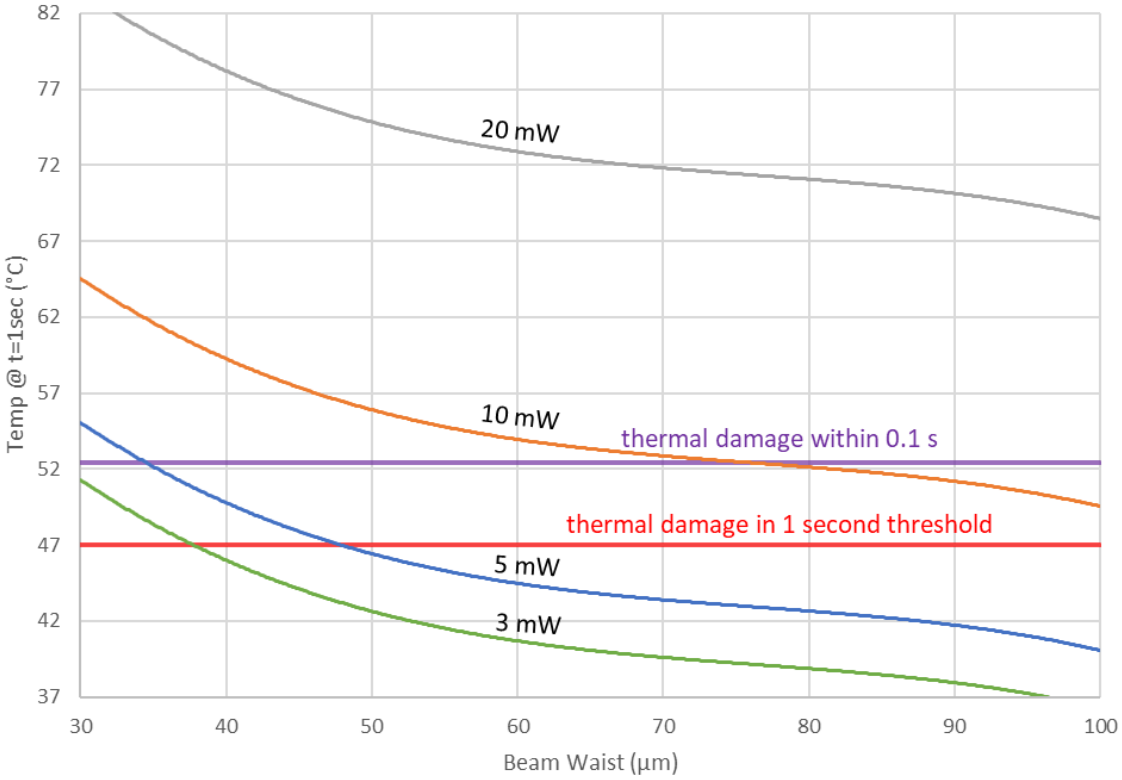

Fig. 26: Peak retinal temperatures after 1 second of heating. This figure shows a prediction of temperature increase after heating. The red horizontal line indicates the thermal damage threshold of an increase of 10°C, known to cause damage to the retina. The purple line indicates this damage can be reached within 0.1 seconds, where the blink reflex may not prevent laser damage.

6 Comparison of 3 different wavelengths

Different laser colors were investigated as an additional part of this report. The three laser wavelengths tested are 650 nm (red), 520 nm (green), and 420 nm (violet). These colors were selected since they are the three most common colors used in handheld laser pointers. An analysis of potential retinal damage was conducted for each wavelength, assuming a 5 mW laser with a 50 μm beam waist for 1 second of heating. Table 2 shows absorbance coefficients of ocular media depending on the chosen wavelength with coefficient of absorption values for the cornea, lens, vitreous humor and retina.

Lower wavelength lasers (violet color) show a lower increase in temperature on the fovea when compared to higher wavelength lasers (green and red). This is mainly because the lower wavelength laser has a 2 times higher absorbance coefficient of the retina than higher wavelength lasers. Also looking at the absorbance coefficient of other ocular media such as the cornea, lens and vitreous humor, the violet laser has a significantly higher value than the lasers in green and red color. For example, in the lens, violet lasers have close to a 10 times greater absorbance coefficient. Therefore, irradiance becomes greatly reduced before it reaches the retina. Hence the temperature increase after 1 sec for the violet color laser is just 2°C, whereas for the red and green color laser the temperature increase is up to 7-10°C (Fig. 27).

In the front portions of the eye, since more of the irradiance is absorbed for the violet wavelength, there is a greater temperature increase in the cornea, lens, and vitreous humor. Figure 28 shows the temperature plots for the surface of the cornea for all three wavelengths. The violet laser has a much greater temperature increase than that of the red and green lasers.

Table 2: Wavelength Dependent Absorbance Coefficients of Ocular Media.

Color/Range	Description	Value	Units	Source
Violet (420 nm)	$\mu_{a\_cornea\_420}$	3.63	1/cm	23
	$\mu_{a\_lens\_420}$	1.92	1/cm	23
	$\mu_{a\_vitreous\_humor\_420}$	0.0684	1/cm	23
	$\mu_{a\_retina\_420}$	4823.221	1/cm	28, 29
Green (530 nm)	$\mu_{a\_cornea\_530}$	1.95	1/cm	23
	$\mu_{a\_lens\_530}$	0.209	1/cm	23
	$\mu_{a\_vitreous\_humor\_530}$	0.0473	1/cm	23
	$\mu_{a\_retina\_530}$	2146.667	1/cm	28, 29
Red (650 nm)	$\mu_{a\_cornea\_650}$	1.41	1/cm	23
	$\mu_{a\_lens\_650}$	0.159	1/cm	23
	$\mu_{a\_vitreous\_humor\_650}$	0.0402	1/cm	23
	$\mu_{a\_retina\_650}$	1055.13	1/cm	28, 29

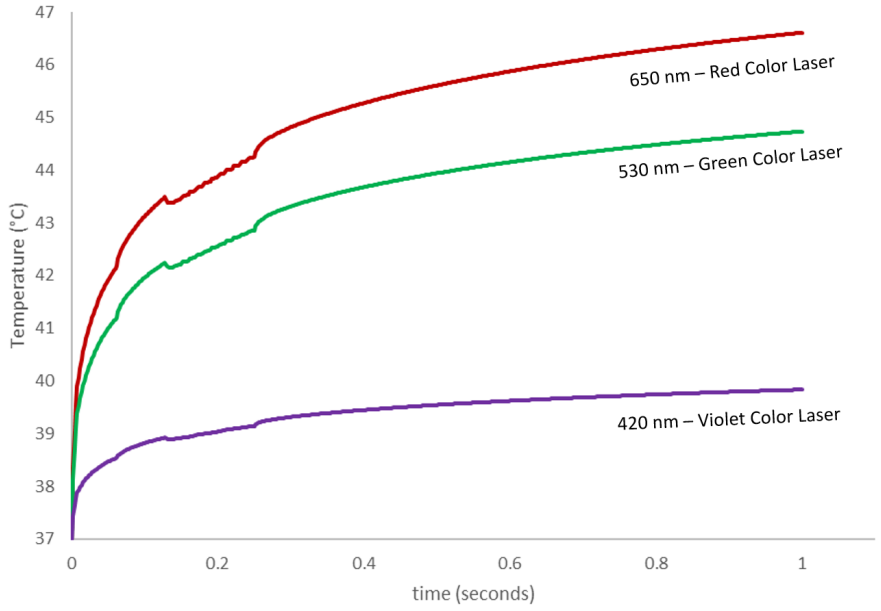

Fig. 27: Peak Retinal temperatures. The image shows retinal Temperature increase over 1 second of 650 (red), 530 nm (green), and 420 nm (violet) colored lasers, all other parameters are consistent. The plot indicates that violet color laser has a lesser increase in temperature on the fovea as compared to green and red color lasers.

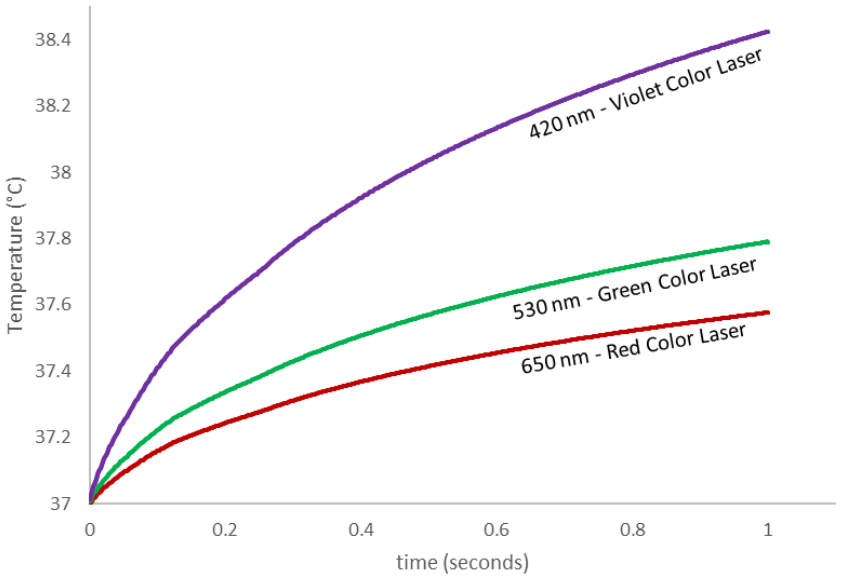

Fig. 28: Peak corneal temperatures: The above plot shows difference in corneal temperature over 1 second for 650 nm (red), 530 nm (green), and 420 nm (violet) colored lasers. Violet colored lasers have higher corneal absorbance coefficient and hence higher temperature increase as compared to red and green colored lasers.

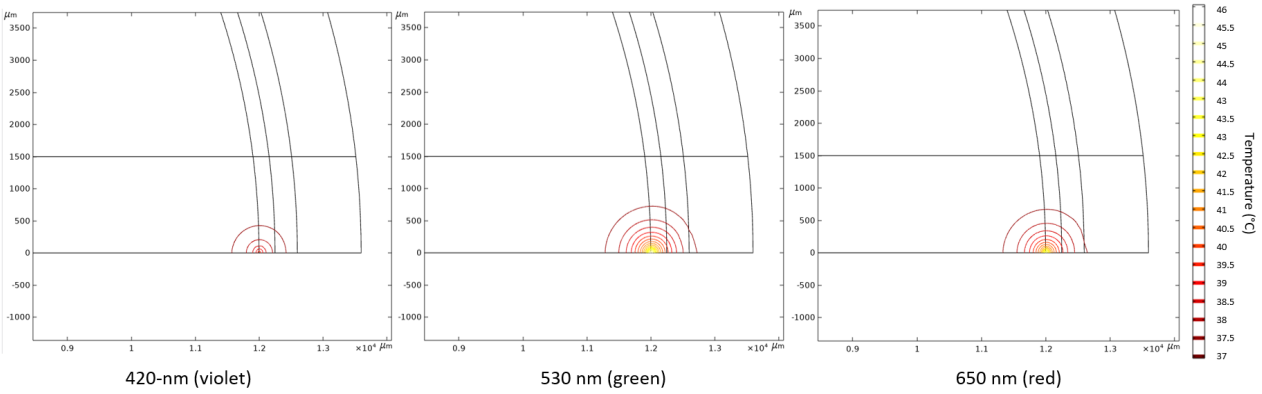

Fig. 29: Contour Plots of violet, green and red colored laser: The temperature increase is small over the fovea region for the violet colored laser as compared to green and red due to reduced irradiance in the retina.

7 Standards for use of Laser Pointers

Laser products promoted for pointing and demonstration purposes are limited to hazard Class IIIa by FDA regulation [2]. According to 21 CFR 1040.11(b) and 1040.11(c) pointers are limited to 5 milliwatts of output power in the visible wavelength range from 400 to 710 nanometers. There are also limits for any invisible wavelengths and for short pulses. Pointers may not exceed the accessible emission limits of CDRH Class IIIa or IEC Class 3R.

7 Appendix A: Table of Input Parameters

All property values to solve our model in COMSOL are listed below:

Table 3: Common laser pointer wavelengths and associated colors.

Color	**Wavelength(s)**
Red	638 nm, 650 nm, 670 nm
Orange	593 nm
Yellow	589 nm, 593 nm
Green	532 nm, 515/520 nm
Blue	450 nm, 473nm, 488 nm
Violet	405 nm

Table 4: Property Values.

Parameter	**Description**	**Value**	**Unit**	**Source**
ρ_{cornea}	Density of tissue	1050	kg/m^3	12
ρ_{lens}		1050		12
$\rho_{vitreous\ humor}$		1000		12
ρ_{retina}		1050		12
$\rho_{choroid}$		1050		12
ρ_{sclera}		1100		12

$c_{p\ cornea}$	Specific heat of tissue	4178	J/kgK	12
$c_{p\ lens}$		3001		12
$c_{p\ vitreous\ humor}$		4178		12
$c_{p\ retina}$		3680		12
$c_{p\ choroid}$		3617		12
$c_{p\ sclera}$		3180		12
$k_{\ cornea}$	Thermal conductivity of tissue	0.58	W/mK	12
$k_{\ lens}$		0.400		12
$k_{\ vitreous\ humor}$		0.603		12
$k_{\ retina}$		0.565		12
$k_{\ choroid}$		0.52		12
Q	Heat generation from light	Eq 6	W/m^3	
$\mu_{a\_cornea\_650}$	Coefficient of absorption	1.055E+03	1/cm	23
$\mu_{a\_lens\_650}$		1.59E-01		23
$\mu_{a\_vitreous\text{-}humor\_650}$		4.02E-02		23
α_{650nm}	Absorption coefficient of retina	1055	1/cm	28, 29
I_0	Incident value of intensity	W/m^2	W/m^2	21
w	Beam waist	50	μm	24
τ	Laser pulse duration	1	ms	
P	Laser power	5	mW	24
λ	Laser wavelength	nm	650	

8 Appendix B: Solution Strategy

CPU Time and memory usage for solving for 1 second of heating is seen in Fig. 30.

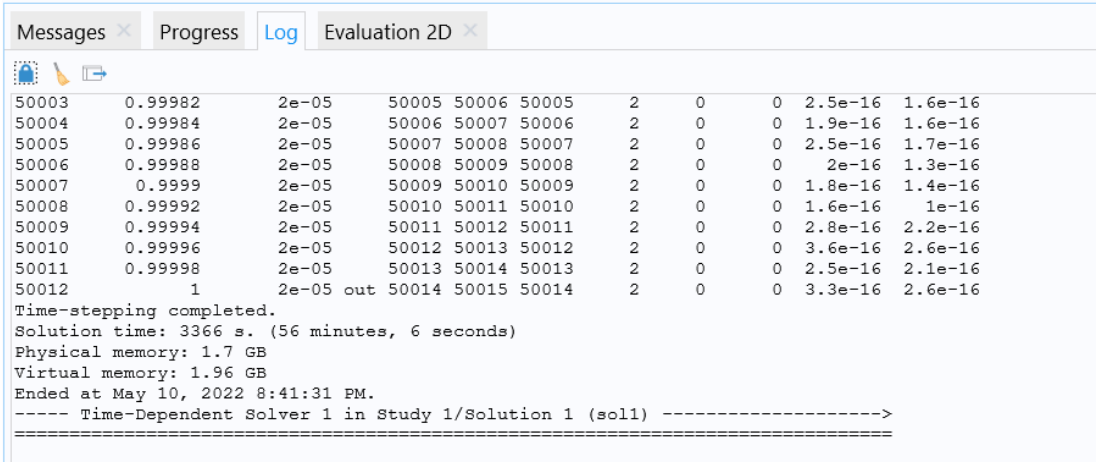

Fig. 30: COMSOL Log for typical solution: 1 second of heating with 1 ms pulse duration

8.1 Computational Methods

Laser Pulses

Modeling laser pulses was a challenge for our computational model, since it requires a periodic function dependent on laser pulse duration. In order to model laser pulses, a sawtooth waveform function (wv1) was created with the following parameters: angular frequency = 2π, phase = π, amplitude = 0.5, as seen in (Fig. 31). Then, a piecewise function was created that contained the equation modeling laser pulses, seen in Eq. 2 of this report. This function utilizes the previous waveform function in order to create a periodic pulse. The equation inputted is:

$$exp(-8((wv1(t)+0.5)^2)/((1)^2),$$

for a 1 ms pulse duration laser. The extrapolation for this waveform should also be periodic. The piecewise function modeling laser pulse can be seen on Fig. 32.

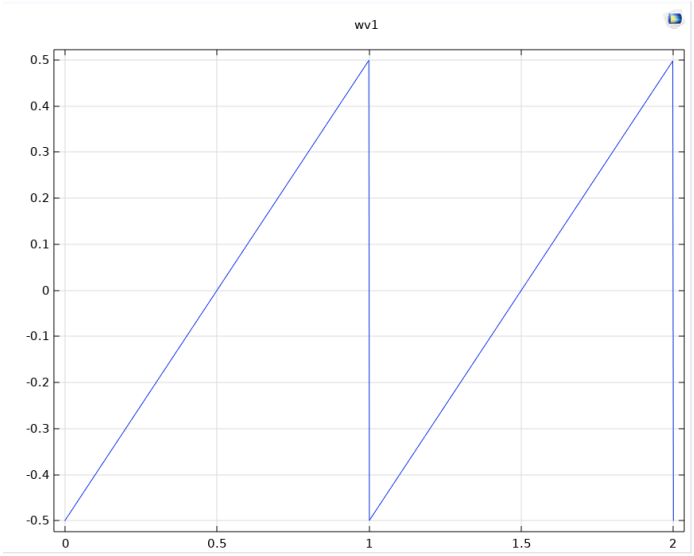

Fig. 31: Sawtooth waveform function used to implement laser pulses

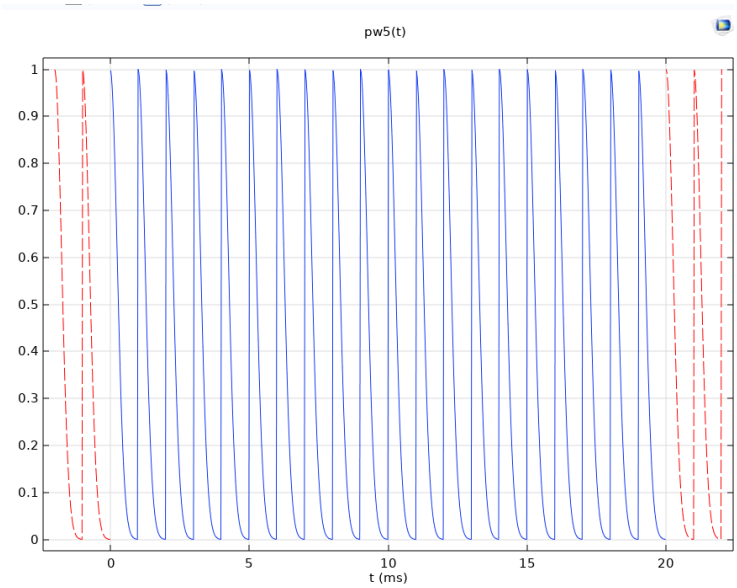

Fig. 32: Piecewise function modeling laser pulses for a pulse duration of 1 ms

Irradiance

For modeling the decay of irradiance through the eye, Eq. 2 can be inputted directly into the Variables section of Definitions. Each region of the eye should have its own Irradiance function, where the I_0 (incident Irradiation) is the Irradiation at the end of the previous domain in which the laser passes. For the cornea, the I_0 is defined by Eq. 3.

The laser pulse portion of the function is implemented by multiplying Irradiance by the piecewise function described in the previous section. In regions other than the retina, Irradiance should appear in a surface plot as a thin beam that decays quickly radially, and decays slower in the z-direction, shown in Figure 33.

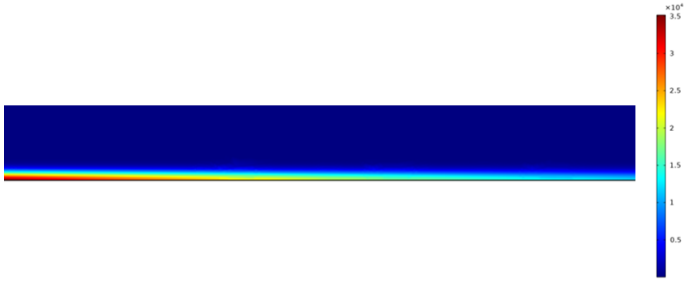

Fig. 33: Typical Irradiance plot for non-retinal ocular media

Miscellaneous Modeling Notes

Pulses may appear to be behaving abnormally when graphing the piecewise function in COMSOL when the pulse number exceeds 100; however, this has been determined to be a plotting error within COMSOL, not an error with the piecewise function.

Due to the curvature of the retina, some portions of the retina may have an abnormally high irradiance. This is because some portions of the retina curve backwards, causing some x-coordinates to become negative. This creates an incorrectly large irradiance due to the expression within the exponential function in Eq. 2 becoming positive. This can be fixed by using the equation of a circle to offset each negative x-value based on the y-coordinate of the retina.

Creating a separate lower and upper region of the geometric model has several benefits. It can allow for localized mesh refinement, shown in Section 4.4, significantly reducing computation time. It can also allow for the irradiance function to only be solved for in these regions, reducing computation as well. However, this region must be much larger than the beam radius to avoid error due to physical approximation.

9 Appendix C: FDA Guidelines on Handheld Laser Pointers

Laser pointers are hand-held lasers that are promoted for pointing out objects or locations [25]. Such laser products can meet one of two definitions for laser products. The first is for "surveying, leveling, and alignment laser products" as defined by Title 21 of the Code of Federal Regulations (CFR) Section 1040.10(b) [39] and hand-held lasers promoted for entertainment purposes or amusement also meet the second definition, that of "demonstration laser products" as defined by 21 CFR 1040.10(b) [13].

Lasers are generally classified according to the hazard posed by the amount and type of light they emit. Hazard classes range from Class I to IV with Class I lasers being non-hazardous and Class IV lasers being the most hazardous.

- Class I products include laser printers and CD players where the laser radiation is usually contained within the product. Products exceeding Class I permit access to some amount of laser radiation.
- Class II and IIa products include bar code scanners.
- Class IIIa products include laser pointers (≤5 mW).
- Class IIIb and IV products include laser light shows, industrial lasers, research lasers (>5 mW).

Laser products promoted for pointing and demonstration purposes are limited to hazard Class IIIa by FDA regulation [25]. 21 CFR 1040.11(b) and 1040.11(c), limit surveying, leveling, and alignment, and demonstration laser products to Class IIIa. This means that pointers are limited to 5 milliwatts output power in the visible wavelength range from 400 to 710 nanometers. There are also limits for any invisible wavelengths and for short pulses. Pointers may not exceed the accessible emission limits of CDRH Class IIIa or IEC Class 3R.

Class IIIa or IEC Class 3R lasers can be dangerous. Class IIIa lasers can cause temporary visual effects such as flash blinding, which could distract or startle the person exposed. The risk of injury is very small when Class IIIa pointers are used responsibly because natural body motion of a person holding the pointer or motion of a person who might be exposed makes it difficult to expose the eyes for a long period of time. People also have a natural aversion to bright lights and are likely to close their eyes and turn their heads if exposed.

10 References

1. OPI Online Courses, *Laser Hazards* http://www.optique-ingenieur.org/en/courses/OPI_ang_M01_C02/co/Contenu_05.html#:~:text=3%20shows%20that%20the%20most,on%20this%20complex%20optical%20element
2. Birtel J, Harmening WM, Krohne TU, Holz FG, Charbel Issa P, Herrmann P. Retinal Injury Following Laser Pointer Exposure. *Dtsch Arztebl Int*. 2017;114(49):831-837. doi:10.3238/arztebl.2017.0831 https://www.ncbi.nlm.nih.gov/pmc/articles/PMC5754573/
3. Environmental Health and Safety, Oregon State University, *Laser Biological Hazards - Eye* Article https://ehs.oregonstate.edu/laser/training/laser-biological-hazards-eyes
4. Datta, Ashim Rakesh, Vineet. (2010). *Introduction to Modeling of Transport Processes - Applications to Biomedical Systems.* Cambridge University Press. Retrieved from https://app.knovel.com/hotlink/toc/id:kpIMTPABS6/introduction-modeling/introduction-modeling
5. Sardar, D.K., Yust, B.G., Barrera, F.J. *et al.* Optical absorption and scattering of bovine cornea, lens and retina in the visible region. *Lasers Med Sci* 24, 839–847 (2009). https://doi.org/10.1007/s10103-009-0677-0
6. Laser Pointer Safety, Laser Classes Chart, https://www.laserpointersafety.com/laserclasses.html
7. Gürsu, Elif & Berberoğlu, Kübra. (2020). Heat and Mass Transfer in the Human Eye. Yildiz Technical University. https://www.researchgate.net/publication/341295014_Heat_and_Mass_Transfer_in_the_Human_Eye
8. Shenoy R, Bialasiewicz AA, Bandara A, Isaac R. Retinal Damage from Laser Pointer Misuse - Case Series from the Military Sector in Oman. *Middle East Afr J Ophthalmol*. 2015;22(3):399-403. doi:10.4103/0974-9233.159780 https://www.ncbi.nlm.nih.gov/pmc/articles/PMC4502191/
9. van Norren D, Vos JJ. Light damage to the retina: an historical approach. *Eye (Lond)*. 2016;30(2):169-172. doi:10.1038/eye.2015.218 https://www.ncbi.nlm.nih.gov/pmc/articles/PMC4763118/#!po=10.0000
10. "LASERS AND OPTICAL RADIATION." *International Programme on Chemical Safety*, World Health Organization, https://inchem.org/documents/ehc/ehc/ehc23.htm
11. "Choroid - An Overview." *ScienceDirect*, Reference Module in Neuroscience and Biobehavioral Psychology, 2017, https://www.sciencedirect.com/topics/veterinary-science-and-veterinary-medicine/choroid

12. Gokul KC et al, Mathematical model: Comparative Study of Thermal Effects of Laser in Corneal Refractive Surgeries https://www.pvamu.edu/sites/mathematics/journal/aam/2015/vol-10-issue-1/37_r715-gokul-vol.-10-issue-1-postes-06-22-15.pdf
13. Sandell JL, Zhu TC. A review of in-vivo optical properties of human tissues and its impact on PDT. *J Biophotonics*. 2011;4(11-12):773-787. doi:10.1002/jbio.201100062 https://www.ncbi.nlm.nih.gov/pmc/articles/PMC3321368/#:~:text=The%20speed%20of%20these%20photons,the%20tissue%20sample%20%5B27%5D.
14. Patel S, Tutchenko L. The refractive index of the human cornea: A review. Cont Lens Anterior Eye. 2019 Oct;42(5):575-580. doi: 10.1016/j.clae.2019.04.018. Epub 2019 May 5. PMID: 31064697 https://pubmed.ncbi.nlm.nih.gov/31064697/#:~:text=A%20figure%20of%201.376%20is,ranged%20from%201.335%20to%201.4391
15. J. Chem. Phys. 104, 6881 (1996); https://doi.org/10.1063/1.471355
16. Modarres-Zadeh, Mehdi Md*; Parvaresh, Mohammad M. Md*; Pourbabak, Sam Md*; Peyman, Gholam A. Md† Accidental Parafoveal Laser Burn From A Standard Military Ruby Range Finder, Retina: Volume 15 - Issue 4 - P 356-358 https://journals.lww.com/retinajournal/Citation/1995/15040/ACCIDENTAL_PARAFOVEAL_LASER_BURN_FROM_A_STANDARD.16.aspx
17. Kearney JJ, Cohen HB, Stuck BE, et al. Laser injury to multiple retinal foci. Lasers in Surgery and Medicine. 1987 ;7(6):499-502. DOI: 10.1002/lsm.1900070611. PMID: 3431326. https://europepmc.org/article/MED/3431326
18. Ng, E.Y.K., and E.H. Ooi. "FEM Simulation of the Eye Structure with Bioheat Analysis." *FEM Simulation of the Eye Structure with Bioheat Analysis*, Computer Methods and Programs in Biomedicine, 6 May 2006, https://www.sciencedirect.com/science/article/pii/S0169260706000708?via=ihub.
19. Peter K.F. Grieder, in Cosmic Rays at Earth, 2001
20. COMSOL Blog, *Modeling Laser-Material Interactions with the Beer-Lambert Law,* by Walter Frei, April 13, 2015 https://www.comsol.com/blogs/modeling-laser-material-interactions-with-the-beer-lambert-law/
21. Mirnezami SA, Rajaei Jafarabadi M, Abrishami M. Temperature distribution simulation of the human eye exposed to laser radiation. *J Lasers Med Sci*. 2013;4(4):175-181. https://www.ncbi.nlm.nih.gov/pmc/articles/PMC4282006/
22. Ven, Sam. "I Have Been Told I Am Not a Candidate for LASIK Because My Corneas Are Too Thin. Does That Mean I Am Stuck in These Glasses and Contact Lenses?" *I Have Been Told I Am Not a Candidate for LASIK Because My Corneas Are Too Thin. Does That Mean I Am Stuck in These Glasses and Contact Lenses?*, Price Vision Group, 15 July 2105, https://pricevisiongroup.com/2015/07/30/i-have-been-told-i-am-not-a-candidate-for-lasik-

because-my-corneas-are-too-thin-does-that-mean-i-am-stuck-in-these-glasses-and-contact-lenses/#:~:text=The%20average%20corneal%20thickness%20is,as%20thick%20as%20630%20microns.
23. Maher, Edward F., Transmission and Absorption Coefficients for Ocular Media of the Rhesus Monkey, Final rept. 15 Sep 1974-15 Sep 1976, SCHOOL OF AEROSPACE MEDICINE BROOKS AFB TX https://apps.dtic.mil/sti/citations/ADA064868
24. Mainster MA, Stuck BE, Brown J. Assessment of Alleged Retinal Laser Injuries. *Arch Ophthalmol.* 2004;122(8):1210–1217. doi:10.1001/archopht.122.8.1210 https://jamanetwork.com/journals/jamaophthalmology/article-abstract/416518
25. US Food and Drug Administration, Important Information for Laser Pointer Manufacturers https://www.fda.gov/radiation-emitting-products/laser-products-and-instruments/important-information-laser-pointer-manufacturers#:~:text=Class%20IIIb%20hand%2Dheld%20lasers,requirements%20and%20United%20States%20law.
26. Operating Instructions, "The Meade Green Laser Pointer" https://www.meade.com/wp/wp-content/uploads/2017/12/Green-Laser-Pointer-Rev-3.pdf
27. "Lasers: Edmund Optics." Gaussian Beam Propagation, Edmund Optics, https://www.edmundoptics.com/knowledge-center/application-notes/lasers/.
28. Jacques, S L, and D J McAuliffe. "The Melanosome: Threshold Temperature for Explosive Vaporization and Internal Absorption Coefficient during Pulsed Laser Irradiation." *Photochemistry and Photobiology*, U.S. National Library of Medicine, June 1991, https://pubmed.ncbi.nlm.nih.gov/1886936/
29. Jacques, Steve. "Melanosome Absorption Coefficient." *Melanosome Absorption Coefficient*, OMLC, https://omlc.org/spectra/melanin/mua.html
30. Gabel, Veit-Peter, et al. " Visible and near Infrared Light Absorption in Pigment Epithelium and Choroid*." *Institut: Institut Für Biomedizinische Optik*, 1978, https://www.bmo.uni-luebeck.de/fileadmin/files/publications/Gabel__1978_Proc._SPIE_Visible_and_near_infrared_light_absorption_in_pigment_epithelium_and_choroid.pdf.
31. Semenyuk, Vladimir. "Thermal Interaction of Multi-Pulse Laser Beam with Eye Tissue during Retinal Photocoagulation: Analytical Approach." *International Journal of Heat and Mass Transfer*, Pergamon, 10 May 2017, https://www.sciencedirect.com/science/article/pii/S001793101730933X#b0075
32. Guo, Ya, et al. "Monte Carlo Model for Studying the Effects of Melanin Concentrations on Retina Light Absorption." *Journal of the Optical Society of America. A, Optics, Image Science, and Vision*, U.S. National Library of Medicine, Feb. 2008, https://pubmed.ncbi.nlm.nih.gov/18246163/
33. Schmidt, Morgan S., et al. "Trends in Nanosecond Melanosome Microcavitation up to 1540 Nm." *SPIE Digital Library*, Journal of Biomedical Optics, 21 Sept. 2015, https://www.spiedigitallibrary.org/journals/journal-of-biomedical-optics/volume-20/issue-

09/095011/Trends-in-nanosecond-melanosome-microcavitation-up-to-1540nm/10.1117/1.JBO.20.9.095011.full?SSO=1